

Classic Interpretation Problems: Evaluating Carbonates

Mahmood Akbar
Mario Petricola
Mohamed Watfa
Abu Dhabi, United Arab Emirates

Mohammed Badri
Mouhab Charara
Cairo, Egypt

Austin Boyd
Denver, Colorado, USA

Bruce Cassell
Roy Nurmi
Dubai, United Arab Emirates

Jean-Pierre Delhomme
Clamart, France

Mike Grace
Dallas, Texas, USA

Bill Kenyon
Ridgefield, Connecticut, USA

Jon Roestenburg
Jakarta, Indonesia

In recent years, there has been a small revolution in our ability to evaluate carbonates. Novel technology and a community of interpreters determined to crack one hard nut are forcing carbonate reservoirs to reveal many of their secrets.

Carbonate reservoirs account for 40% of today's hydrocarbon production, and because of several elephant fields in the Middle East they are expected to dominate production through the next century. Therefore, understanding carbonate reservoirs and producing them efficiently have become industry priorities and are likely to remain so.

Current efforts in carbonate exploitation focus on correctly targeting new wells, frequently horizontal, to optimize production from untouched reserves and on ensuring that massive water injection schemes deliver an effective sweep of the reservoir. In support of these efforts, geoscientists are trying to decipher the enigma of carbonate rock's complex pore space and understand how permeability barriers and conduits affect

reservoir behavior. This article tracks the interpretation process, from carbonate rock description and petrophysical log evaluation to new techniques for measuring permeability downhole and mapping large-scale flow conduits and barriers.

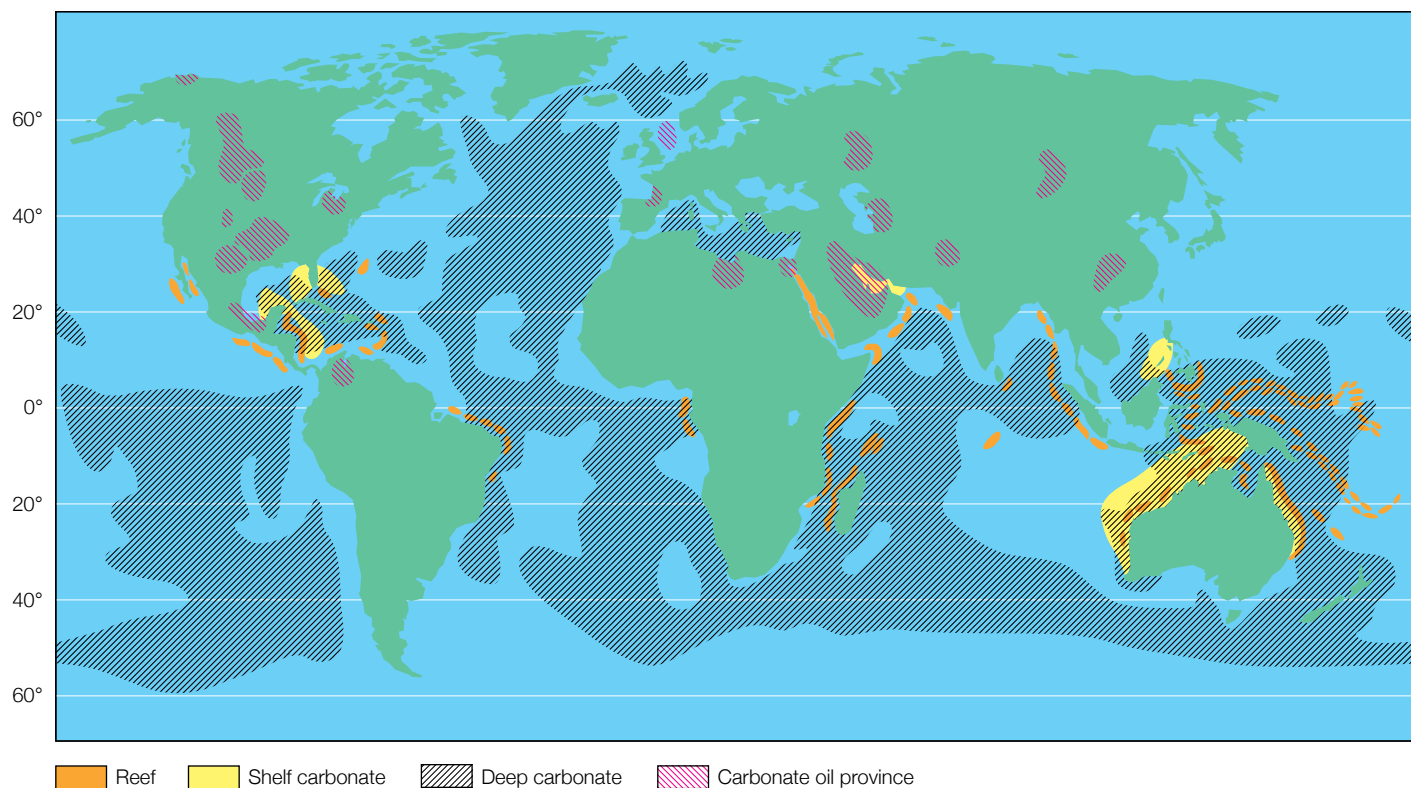
Carbonates for Beginners

Carbonates and sand-shale rocks, or siliciclastics, are worlds apart. Whereas siliciclastic rocks are composed of a variety of silica-based grains that may have traveled hundreds of miles from their source, carbonate rocks mainly consist of just two minerals—calcite and dolomite—and remain near their point of origin.¹ Carbonates form in shallow and deep marine settings, evaporitic basins, lakes and windy deserts.² Most of the carbonates formed in past have shallow

For help in preparation of this article, thanks to Hervé Anxionnaz, Schlumberger Wireline & Testing, Clamart, France; Jean-Louis Chardac, Schlumberger Wireline & Testing, Dubai, UAE; Bob Dennis, Schlumberger Wireline & Testing, Wathayh, Oman; Philip Cheung, Arnaud Etchecopar and Ollivier Faivre, Schlumberger Wireline & Testing, Clamart, France; Brian Hornby, Schlumberger Cambridge Research, Cambridge, England; Rachel Kornberg, GeoQuest, Gatwick, England; William Murphy and Pabitra Sen, Schlumberger-Doll Research, Ridgefield, Connecticut, USA; Oberto Serra, Consultant, Paris,

France; Julian Singer, Schlumberger Wireline & Testing, New Delhi, India; and Eric Standen, Schlumberger Wireline & Testing, Montrouge, France.

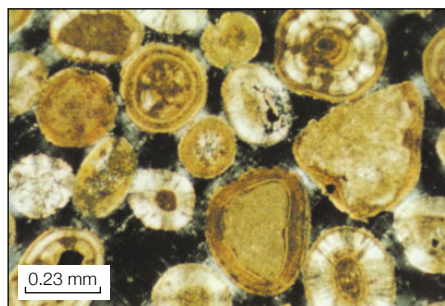
In this article, ARI (Azimuthal Resistivity Imager), CMR (Combinable Magnetic Resonance tool), DSI (Dipole Shear Sonic Imager), EPT (Electromagnetic Propagation Tool), FMI (Fullbore Formation MicroImager), FracView, GeoFrame, MDT (Modular Formation Dynamics Tester) and TDT (Thermal Decay Time) are marks of Schlumberger.



□ **Distribution of carbonates.** Areas of modern sediments in shallow water are shown in yellow and orange, modern deepwater sediments in black-hatched lines. Prolific carbonate oil basins are shown in red-hatched lines. [Adapted from Wilson, reference 2; Blatt H, Middleton G and Murray R: *Origin of Sedimentary Rocks*. Englewood Cliffs, New Jersey: Prentice-Hall, Inc. (1972): 410; and Perrodon A: *Dynamics of Oil and Gas Accumulations*. Pau, France: Bulletin des Centres de Recherches Exploration-Production Elf-Aquitaine (1983): 215.]

marine origins, but the most widespread type of modern carbonate is formed in deep water (*above*). Silica-based rocks generally stand up to the rigors of geologic time, undergoing only minor alteration, or diagenesis. Their depositional record is preserved, with bedding planes on outcrops and subsurface correlations between wells clearly recognizable. The grains are regularly shaped, and the pore space, though complicated, remains intergranular.

Carbonate rocks, on the other hand, are chemically unstable and undergo substantial alteration such as mineral dissolution and dolomitization—the replacement of calcium carbonate by magnesium carbonate. Carbonates house a jumble of complex particles, including a huge variety of biological origin, and an even more complex pore space (*Photographs, reprinted with permission from Scholle, reference 3, are positioned throughout this article*).³ This complicates the tracking of facies across a carbonate reservoir and the assessment of the productivity of a given carbonate formation.



□ **Unfilled interparticle porosity (black).** **Holocene oolite, Great Salt Lake, Utah, USA. Cross-polarized light photograph.**

The typical carbonate rock is made of grains, matrix and cement. Grains are either skeletal fragments of small organisms or particles precipitated from calcium-rich water. The latter includes a variety of small, accretionary grains identified according to their size, origin and internal structure.

Matrix is the lithified mud of deposition that fills most of the space not occupied by grains. In carbonates, fine mud has several sources—chemical precipitation, breaking of skeletal material into finer material,

1. An exception is the less-abundant class of rocks called calcareous sandstones, or carbonate arenites, which form when carbonate rock is broken up by wind or water, then transported and deposited. Calcareous sandstones exhibit many of the structural and petrophysical characteristics of siliciclastic sandstones, while retaining carbonate mineralogy and microporosity.
2. For a review of carbonate geology:
Wilson JL: *Carbonate Facies in Geologic History*. Berlin, Germany: Springer-Verlag, 1975.
Reeckmann A and Friedman GM: *Exploration for Carbonate Petroleum Reservoirs*. New York, New York, USA: John Wiley & Sons, 1982.
Tucker ME and Wright VP: *Carbonate Sedimentology*. Oxford, England: Blackwell Scientific Publications, 1990.
3. Scholle PA: *A Color Illustrated Guide to Carbonate Rock Constituents, Textures, Cements and Porosities*. Tulsa, Oklahoma, USA: American Association of Petroleum Geologists, 1978.

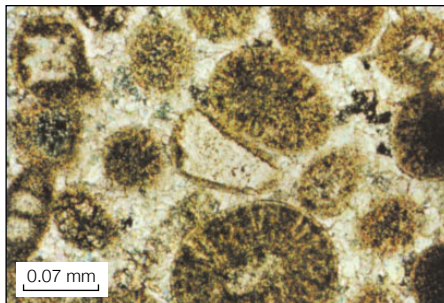
remains of algae, and others. On lithification, mud becomes a very fine-grained calcite called micrite.

Cement describes crystalline material that forms in most of the space remaining between grains and matrix or between grains themselves, binding them. Cement may have a variety of crystal sizes depending on its composition, the conditions of crystallization and the spaces to be filled.

Crucial to the interpretation of carbonates is classifying the numerous ways grains and matrix coexist. Progress in categorizing these complexities surged in the late 1950s because of pressure within oil companies to better understand their carbonate assets. The classification that has stood the test of time most successfully is by Robert Dunham.⁴

Dunham classifies a spectrum of rock types based on the internal structure and texture of the rock (*below*). Mudstone consists mainly of matrix in which relatively few grains are suspended. Wackestone is also matrix-supported but has more grains. Packstone has enough grains for them to start providing support—matrix fills the remaining nonpore space. Grainstone has plenty of grains providing support and includes progressively less matrix. Finally, boundstone describes carbonate rocks in which the original material provided support during deposition, such as in reefs. Crystalline describes rock that has lost its depositional fabric because of diagenetic recrystallization, for example, dolomitization.

Dunham's classification provides some clue to the energy of deposition. The mud-based mudstone and wackestone are



□ **Calcite-filled interparticle porosity (black) in oolite. Upper Mississippian Pitkin Limestone, Oklahoma, USA. Cross-polarized light photograph.**

deposited in low-energy settings. Packstone and grainstone would appear to be from high-energy deposition, but given significant diagenesis, these grain-supported rocks could equally well have been deposited as mud-supported agglomerations and then through compaction and chemical alteration transformed to their present state. The difficulty in classifying carbonates to reflect both their current state and depositional history demonstrates how dominant diagenesis is in forming the final carbonate rock.

Diagenesis may be divided into five main mechanisms: *compaction*—the reduction of pore space in response to tighter grain packing as overburden increases; *carbonate degradation*—the destruction of carbonate material through chemical dissolution and micritization, the transformation of large crystals into small ones; *carbonate aggradation*—the construction of carbonate material through precipitation of cement between grains, and recrystallization, such as the

replacement of limestone by dolomite; *stylolization*—the formation of stylolites, irregular planes of discontinuity between rock units due to compaction-related pressure solution; and *fracturing*—the planar breaking up of rock mass due to stress.

Time and diagenesis generally work against the preservation of porosity (*next page*). Young carbonates usually have porosities around 60%. Old carbonates have just a percent or two. Reservoir carbonates survive with porosities of 5 to 15% largely because the presence of hydrocarbon impedes further destruction of porosity. The typically prolonged and extensive diagenesis in carbonates also usually obscures the provenance and history of the rock.

Reservoir Description

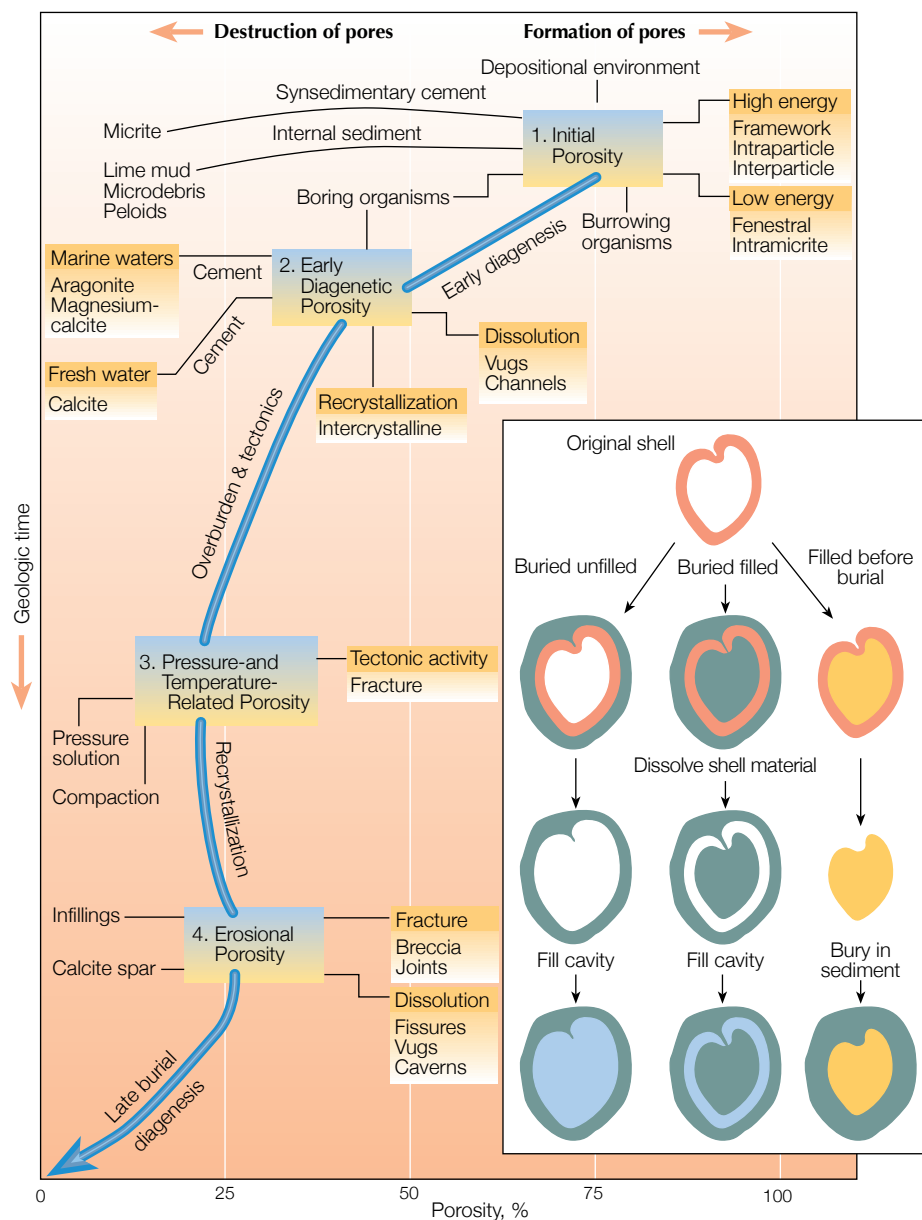
How does the reservoir geologist use these descriptions to help plan the optimum exploitation of a carbonate reservoir? Identifying and classifying carbonates are crucial in two key tasks. First, assessment of the reservoir's paleoenvironment builds a broad understanding of likely reservoir geometry. Then, detailed well-to-well correlation of lithofacies helps construct a detailed three-dimensional picture.

Clues to paleoenvironment come from every available source—seismic surveys, outcrop studies, cuttings and core analysis, and logs, including those from the latest generation of electrical imaging tools, which can capture the wellbore likeness to a resolution of about 5 mm [0.19 in.] The main paleoenvironment indicators are:

- **Lithology**—This provides a general idea of the depositional setting. The presence of clastic rocks indicates an external source of sediment, while their absence indicates an environment free of external influence.
- **Rock texture**—The Dunham classification of texture provides some idea of the energy of deposition. Grain size variations also point to the sequence of deposition. For example, a fining upward sequence may indicate a relative sea level rise, or marine transgression. A coarsening upward sequence probably indicates a relative sea level drop.
- **Sedimentary structure**—Large-scale sedimentary structures are more difficult to see in carbonates than in siliciclastics, but when identified, they offer powerful clues to the depositional environment. Examples are crossbeds in eolian dunes or solu-

Mudstone	Wackestone	Packstone	Grainstone	Boundstone	Crystalline
Less than 10% grains	More than 10% grains	Grain-supported	Lacks mud and is grain-supported	Original components were bound together	Depositional texture not recognizable
Mud-supported					
Contains mud, clay and fine silt-size carbonate					
Original components not bound together during deposition					
Depositional texture recognizable					

□ **Dunham's classification of carbonates, based on the internal structure of the rock.**



tion grooves caused by irregular dissolution of the surface of a carbonate rock.

- **Biofacies**—Identification of the wide variety of skeletal grains, burrows and molds may pinpoint precise geological time and settings. Ages and habitats of hundreds of carbonate creatures have been tabulated for this purpose.

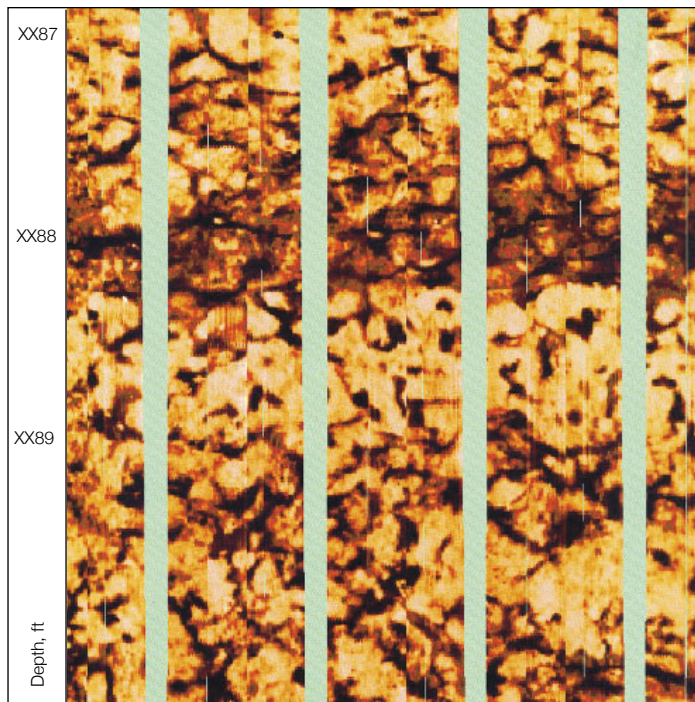
- **Nonskeletal content**—Grains formed by precipitation and accretion provide a powerful indicator of depositional setting. For example, homogeneous pellets develop in quiet lagoons, while concentrically layered ooids occur mainly in active, shallow environments.

- **Authigenic minerals**—The cement and minerals that form in the rock after deposition provide some additional clues. The presence of pyrite suggests reducing (deoxidizing) conditions; glauconite indicates marine conditions; organic matter indicates little reworking.

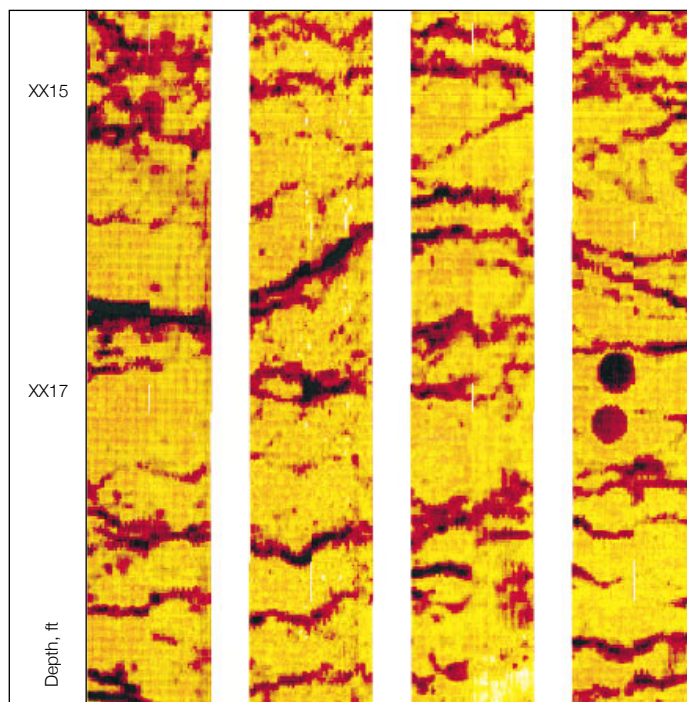
Slowly evidence accumulates, and the origin and evolution of the reservoir become less conjectured and more certain. In comparison, the mapping of lithofacies is a detailed, nuts-and-bolts task, but no less challenging. Unlike siliciclastics, carbonates usually carry no bedding signatures that allow ready well-to-well correlation across a field. Even dipmeter correlations across the borehole can be elusive. There are exceptions. Eolian carbonate deposits, for example, display continuity and bedding signatures exactly like their siliciclastic equivalents. More frequently, though, carbonates exhibit a mix of features such as fractures, breccia, stylolites and vugs.

Helping the reservoir geologist recognize and catalog these features in wells drilled

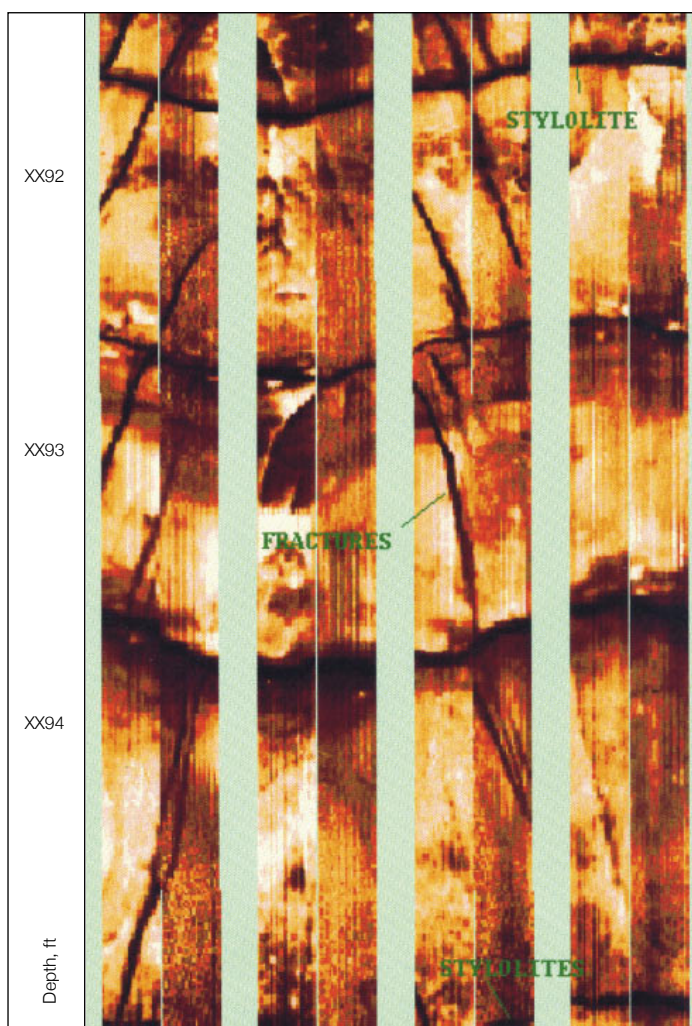
4. Dunham RJ: "Classification of Carbonate Rocks According to Depositional Texture," in Ham WE (ed): *Classification of Carbonate Rocks*. Tulsa, Oklahoma, USA: American Association of Petroleum Geologists, 1962.



□ **Mottled fabric with thin producing zone at XX88 ft. Dark color is interpreted as mud-filled porosity. Light color is grains and matrix.**



□ **Swarms of stylolites in a Mississippian carbonate, with two core points visible.**



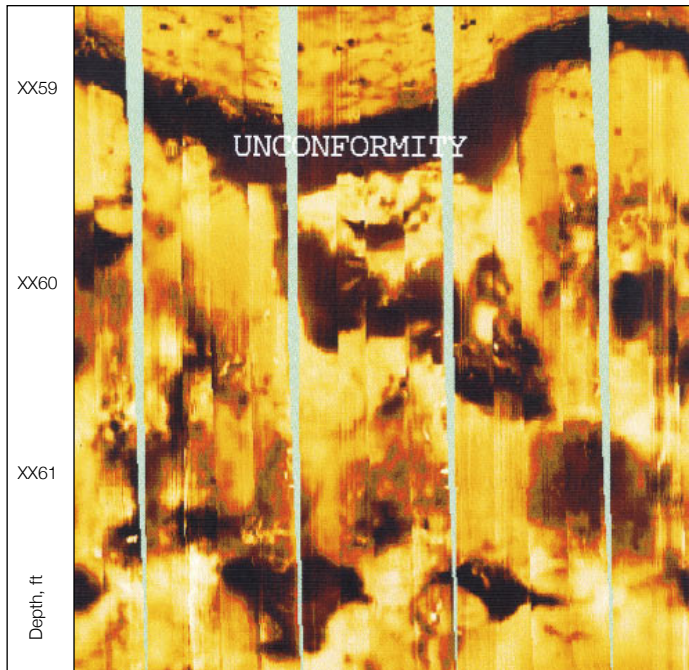
□ **Subhorizontal stylolites (wide dark bands) and inclined fractures (narrow dark lines) in a Middle East carbonate formation.**

with water-base mud is the FMI Fullbore Formation MicroImager tool, which provides a picture of most of the borehole with 192 small current-emitting buttons mounted on four pads and four flaps. In the images, light color denotes high resistivity, indicating rock grains or hydrocarbon-filled pores, and dark color indicates low resistivity such as water-filled pores or shale. The images are no substitute for core analysis, but rather a complement to them. Other evidence is frequently needed to corroborate an interpretation, for example to decide whether a dark patch is porosity or shale. However, an experienced interpreter of FMI images can glean strong evidence of numerous types of carbonate features down to the centimeter scale (*this page and next page*).⁵

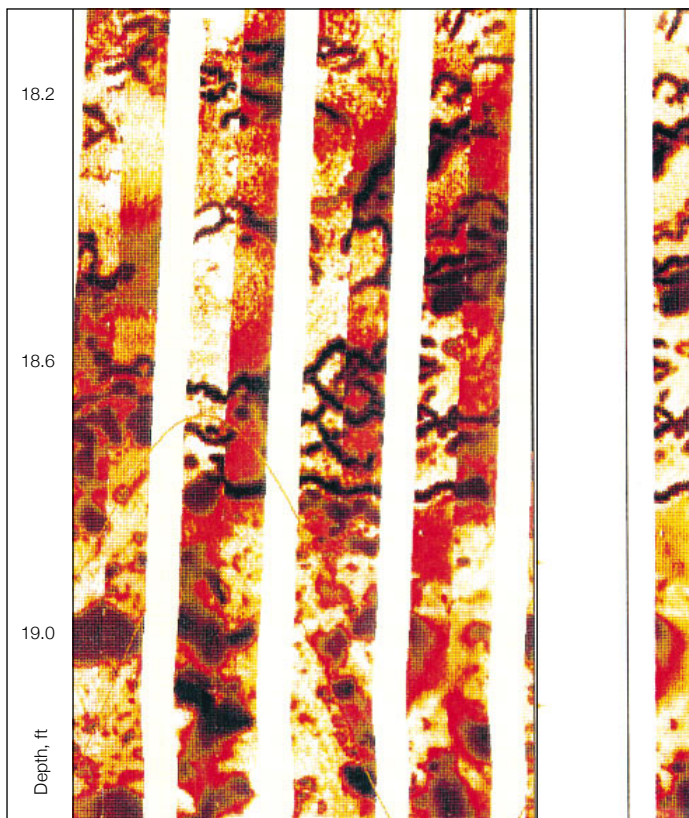
A recent trend in FMI interpretation has been toward quantitative analysis of the images. One processing method automatically extracts five facies types based on a textural classification by Nurmi et al.⁶ The facies are *uniform* zones of constant conductivity or resistivity; *layered* zones of alternating conductive and resistive layers; zones

5. Serra O: *Formation MicroScanner Image Interpretation*. Houston, Texas, USA: Schlumberger Educational Services, 1989.

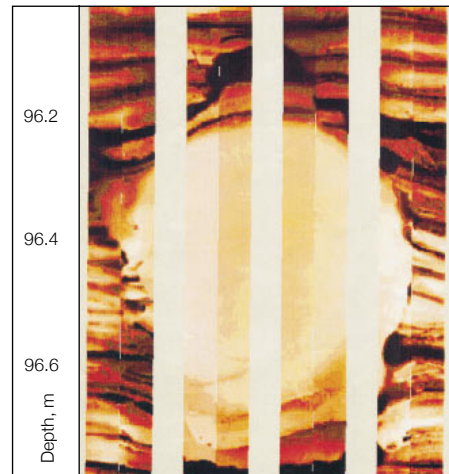
6. Nurmi R, Charara M, Waterhouse M and Park R: "Heterogeneities in Carbonate Reservoirs: Detection and Analysis Using Borehole Electrical Imagery," in Hurst A, Lovell MA and Morton AC (eds): *Geological Applications of Wireline Logs*. London, England: Geological Society of London, 1990.



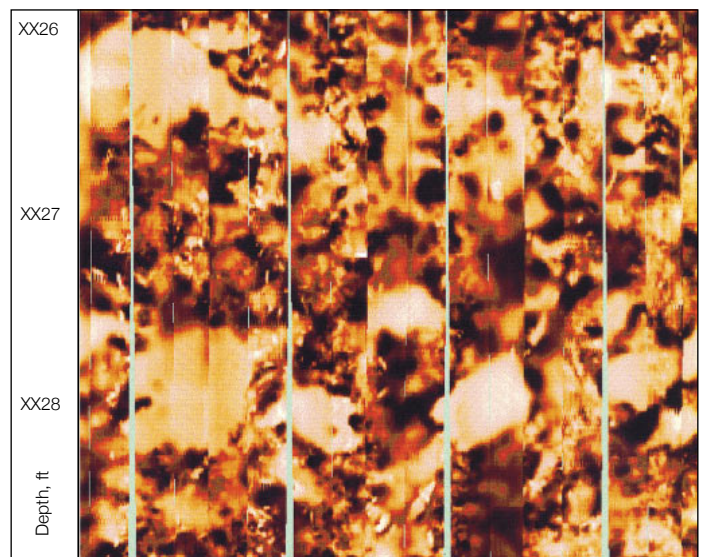
□ **Unconformity between overlying shale and mid-Cretaceous carbonate. Large, irregular dark features below the unconformity are voids created by extensive dissolution during subaerial exposure.**



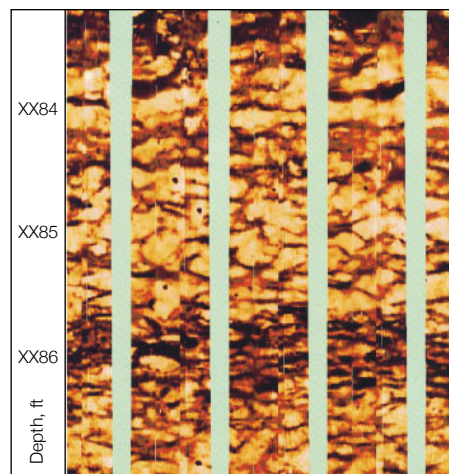
□ **Breccia caused by collapse of a limestone cavern, indicated by interconnected channels between sharp fragments of rock. This type of breccia porosity often makes for prolific production.**



□ **Large calcite concretion, that may help elucidate depositional environment.**



□ **Secondary micrite formation in the form of large, light-colored areas.**



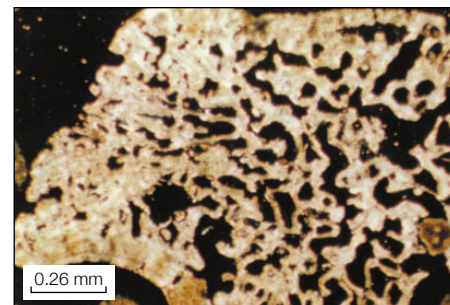
□ **Mottled fabric of an Upper Cretaceous carbonate reservoir in the Middle East.**

with *interwoven* or contiguous conductive areas, interpreted as interconnected porosity; resistive zones with *isolated conductive* areas, interpreted as nonconnected pores; and conductive zones with *isolated resistive* areas, caused for example by nonconducting calcite or anhydrite nodules. Such a zonation can be rapidly calculated from the images and lends itself readily to facies mapping across a field (*below*).

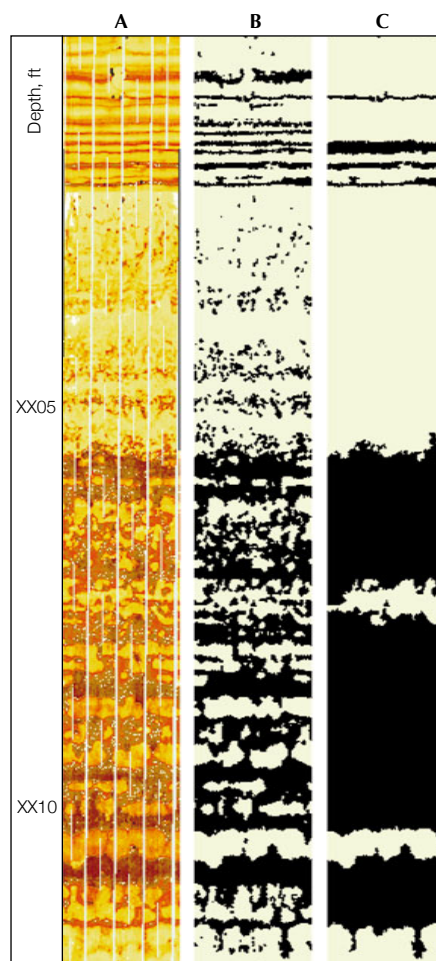
A more advanced processing method actually delineates identifiable objects such as rock grains or pores on the images.⁷ This is quite a challenge because picking the edge of an object depends somewhat on overall image intensity, which varies. The solution is to equate object boundaries with inflection points in image intensity. This approach is incorporated in SPOT—Secondary Porosity Typing—prototype software running on Geo-

Quest's GeoFrame platform. Current SPOT processing can yield the boundaries of both resistive (light color) and conductive (dark color) features (*next page, top*). In tests made on laboratory rock samples bored with "pores" of varying but precisely known diameter, the processing has given accurate and consistent pore delineation.

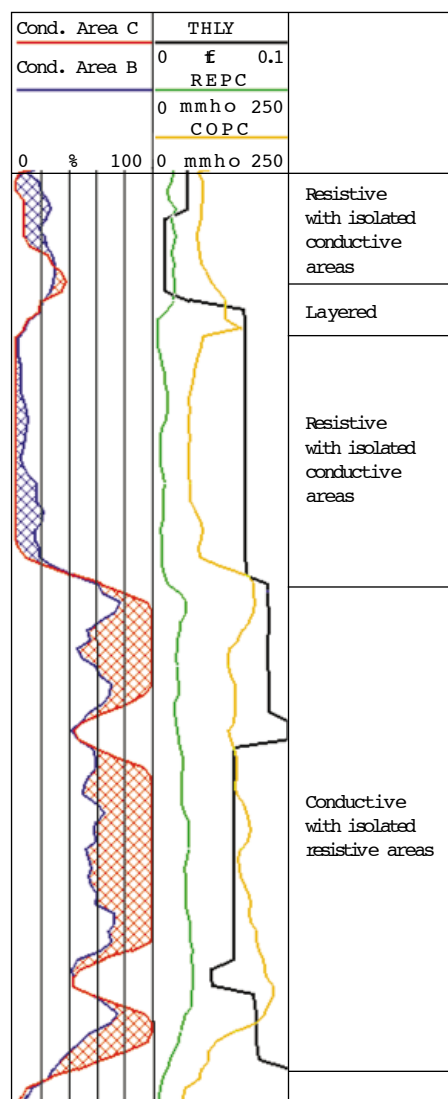
Once resistive and conductive features are delineated, then all manner of quantitative information can be computed, such as their average size, the spatial density of the features, the total area on the image covered by the features, and the degree to which like features are connected. We will later



□ **Unfiled intraparticle porosity (black) within a large coral fragment. Holocene back-reef beach sediment, Belize, British Honduras. Cross-polarized light photograph.**



□ **Implementation of Nurmi's porosity classification through automatic processing. The FMI image is processed to yield resistive and conductive segments (B). Segments that are not continuous across the image are eliminated (C). Conductive area within each processed image is plotted as a log (blue for B, red for C). Average conductivity for resistive segments in B (green) and for conductive segments in B (orange) are shown with the variation in thickness of these segments across the image width (black).**



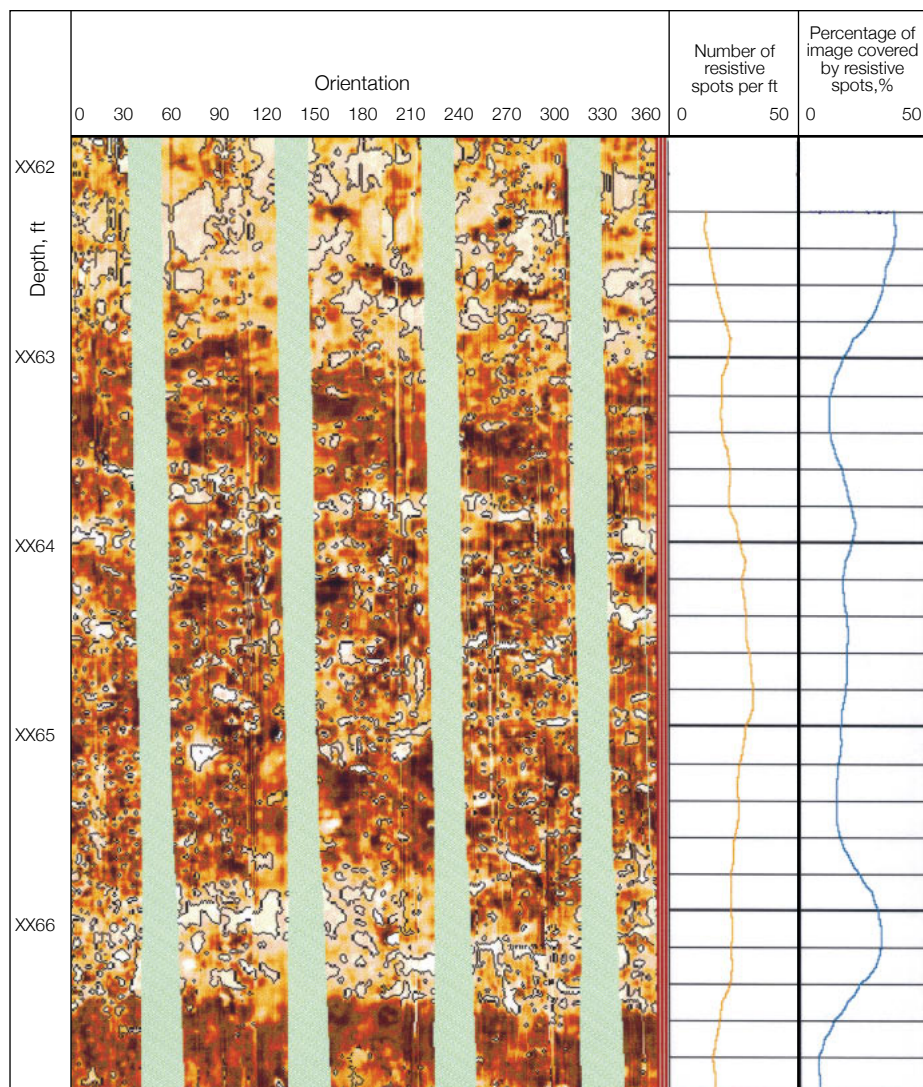
address how these new parameters may contribute to understanding of rock porosity and permeability.

The average sizes of resistive and conductive features have recently been used to help identify Dunham rock types in an Occidental Oil Company field in Indonesia and thus contribute to facies mapping (*page 46, bottom*).⁸ In this interpretation, resistive features correspond to carbonate coral framework or grains, while conductive features correspond to pores or micritic matrix. On a log, the average sizes of the two types of features are played back together. The interpretation proceeds by noting the separation between the curves and also their absolute magnitudes.

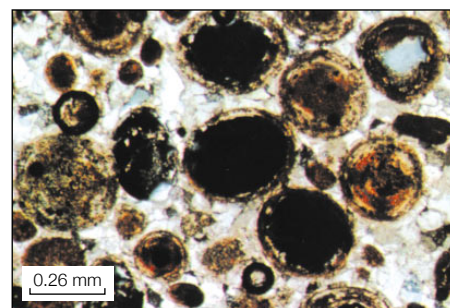
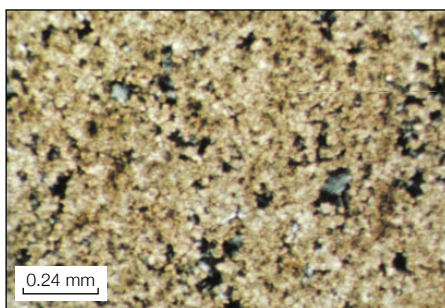
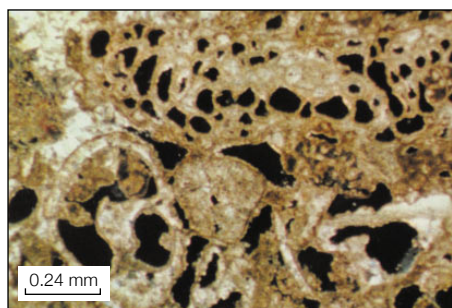
Mudstone is interpreted when separation is at a maximum. This occurs when the average size of conductive features peaks—that is, micritic cement dominates—and the average size of resistive features—or grains—drops. Wackestone is interpreted when the average size of resistive features increases, while the average size of conductive features remains about the same. Packstone is interpreted when the average size of resistive features peaks. And finally, grainstone is interpreted when the sizes of conductive and resistive features become equal. This broad-brush methodology has been verified against macrofacies descriptions from cores in two wells in the field. Furthermore, the frequency with which the two curves mirror one another appears to indicate the frequency of a complete depositional cycle—from low-energy mudstone to high-energy grainstone.

7. Delhomme JP: "A Quantitative Characterization of Formation Heterogeneities Based on Borehole Image Analysis," *Transactions of the SPWLA 33rd Annual Logging Symposium*, Oklahoma City, Oklahoma, USA, June 14-17, 1992, paper T.

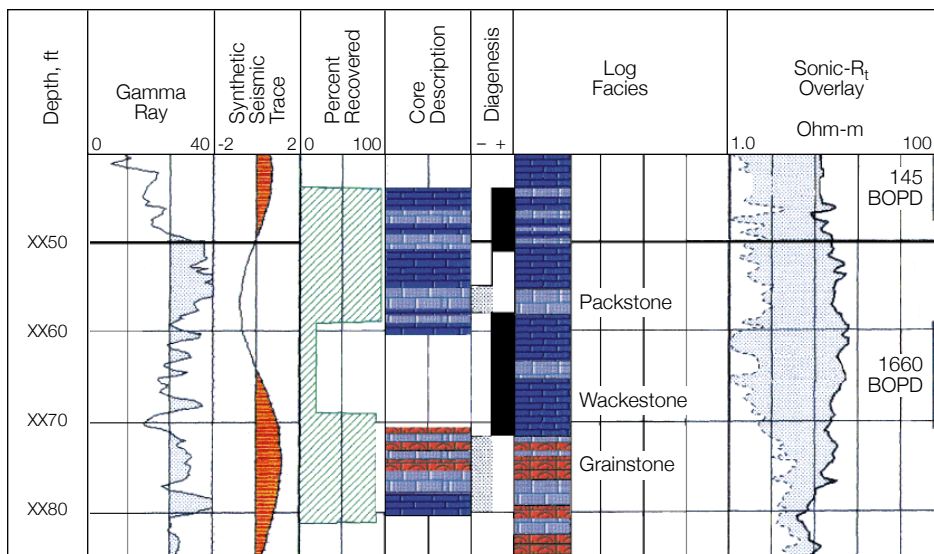
8. Roestenburg JW: "Carbonate Characterization and Classification from In-Situ Wellbore Images," presented at the 23rd Annual Convention of the Indonesian Petroleum Association, Jakarta, Indonesia, October 4-6, 1994.



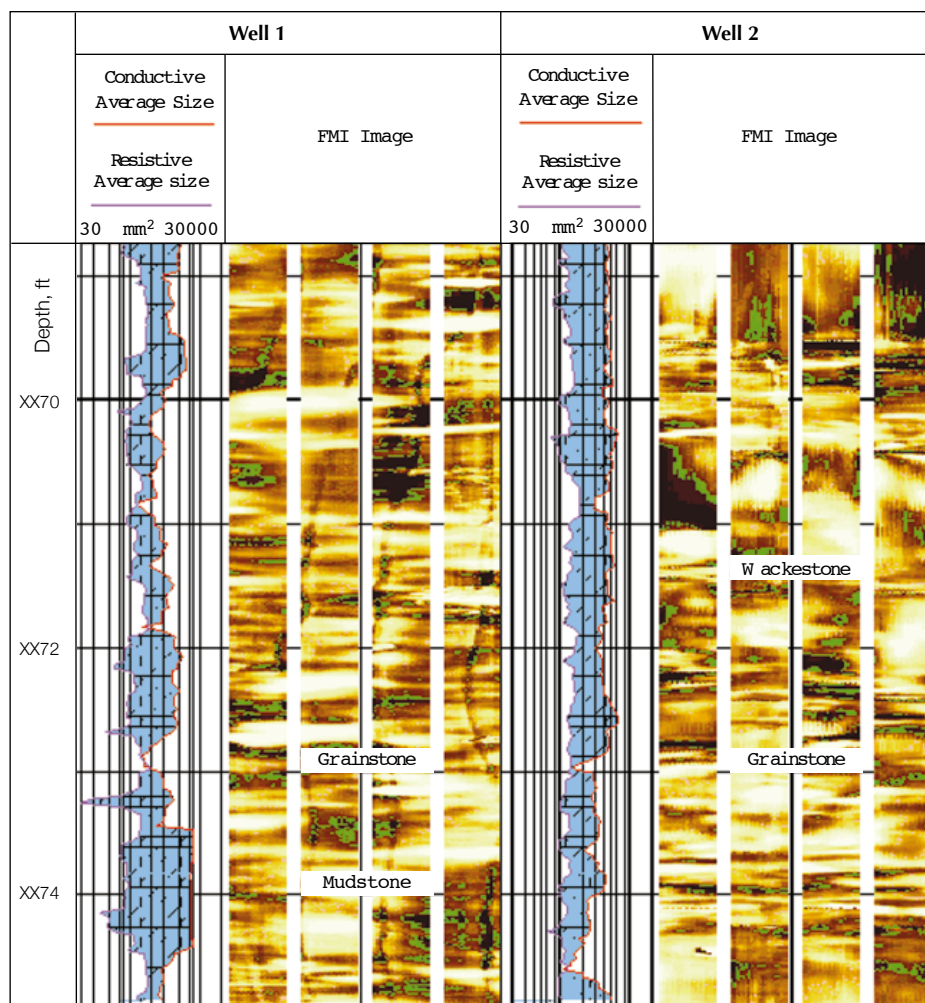
□ **SPOT processing on FMI images delineates either resistive or conductive inclusions, or spots. The inclusions can then be analyzed to provide quantitative parameters such as median size of inclusion, density of inclusions per foot or meter, average area percentage of inclusions, and even a porosity estimate and connectivity parameter.**



□ **Cross-polarized light photographs showing porosity. Left: Reduced interparticle and intraparticle porosity (black) in foraminifera and mollusks. Pleistocene Key Largo Limestone, Florida, USA. Middle: Intercrystal porosity (black) in a fine- to medium-crystalline replacement dolomite. Middle Eocene Avon Park Limestone, Florida. Right: Moldic porosity (black). Pleistocene Miami oolite, Florida.**



□ **Facies interpretation according to Dunham's classification using statistical calibration between log data and petrologic analysis from cores in an offshore carbonate field, India. The calibration allows facies to be mapped across the field using other logged wells without cores.**



□ **Facies interpretation in an Occidental Oil Company carbonate field in Indonesia using SPOT processing to automate Dunham's classification from FMI images. Dunham rock type is interpreted by comparing the relative magnitudes of the average size of resistive and conductive inclusions. Interpretation has been verified from cores.**

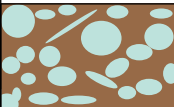
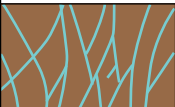


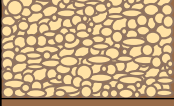

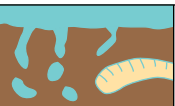




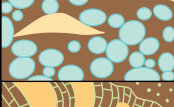



Without images, mapping facies following gamma ray and other log signatures can often prove unreliable. The safest bet, short of coring every borehole, is to collectively interpret all available log data, initially calibrating the interpretation results to core data. An example of this approach can be found in a study by the Indian Oil and Natural Gas Commission (ONGC) and Schlumberger that recently addressed a complex Middle Eocene carbonate formation in offshore India.⁹

In this study, the first step was to identify facies in the four cored wells according to Dunham's classification. This required the analysis of 120 thin sections, 12 polished sections and 6 scanning electron microscope images. This petrologic interpretation was then integrated statistically with five log measurements made in the same wells—density, neutron porosity, sonic travel time, gamma ray and saturation. Matching the log measurements to the facies descriptions revealed clear links between weighted combinations of log data and the Dunham classification (*above, left*). However, rather than Dunham's four, the logs recognized five facies types, the last of which always occurred within a wackestone zone but at depths where no core was retrieved. This facies was termed wackestone+. With logs calibrated to a core facies description, a facies interpretation could be made directly from logs in all the remaining uncored wells, and then facies mapped between wells.

Petrophysical Evaluation

Facies determination from logs is hard enough, but the challenge of establishing petrophysical parameters such as saturation and permeability is even more daunting. The reason lies squarely with the complex diagenesis and resulting convoluted pore systems of most carbonate rocks. Log analysts divide porosity into primary and secondary components, with primary existing at the time of rock formation and secondary appearing as the rock matures and diagenesis prevails. The more detailed classification of Choquette and Pray exposes the immense diversity in both shape and size of carbonate pores (*next page, top*).¹⁰

The variety in pore type explains why permeability answers remain so elusive. Vugs and their cousins may make for high porosity, but a consistent pore connectivity, usually taken for granted in sandstones, may or may not be present. Worse yet, the chaos

Fabric-selective		Not fabric-selective		Fabric-selective or not	
	Interparticle		Fracture		Breccia
	Intraparticle				
	Intercrystal		Channel		Boring
	Moldic		Vug		Burrow
	Fenestral				
	Shelter		Cavern*		Shrinkage
	Growth-framework	*Cavern applies to man-sized or larger pores of channel or vug shapes			

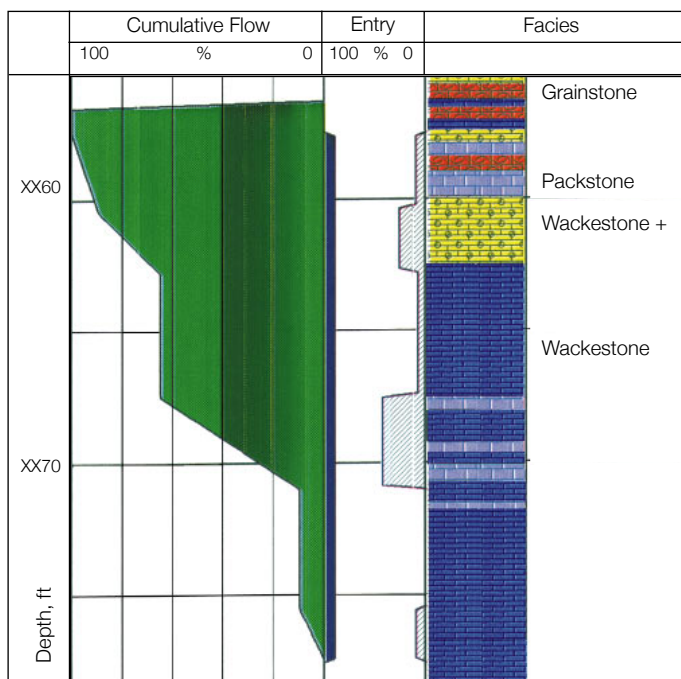
□ **Choquette and Pray's classification of carbonate porosity:** Fabric-selective porosity includes interparticle porosity occurring between grains; intraparticle porosity occurring within original skeletal grains; intercrystal porosity occurring within crystallized micrite and/or dolomite; moldic porosity that results from the dissolution of grains; large-scale framework porosity called fenestral porosity that usually results from dissolution of algal mat deposits; shelter porosity that describes pore space resulting from shelter offered by large overlying grains; and growth-framework porosity that is the natural outcome of organic processes such as coral reefs.

Nonfabric-selective porosity includes fracture porosity; channel porosity caused by extensive leaching; vug porosity that results from extensive dissolution of material and retains no evidence of the original host grain; and man-size cavern porosity that results from highly extensive and prolonged leaching. Porosity that could fall in either camp includes breccia, boring, burrowing and shrinkage porosity.

reigns at all scales. In sandstones, small 1/2-in. [1.27-cm] plugs bored from cores usually provide samples homogeneous enough for estimating average permeability. In carbonates, however, sometimes not even a whole piece of core can be regarded as representative. The discrepancy between permeabilities measured at different scales may be related to heterogeneity or to anisotropy.¹¹ The only sure way of estimating reservoir-scale permeability is by using wireline, drillstem or production tests. This was the approach taken in the second phase of the Indian study, in which nine well tests in two wells established a link between carbonate facies type and permeability.

Each carbonate facies type was allowed a permeability value, to be determined. Then, for each test, the well's flow capacity calculated during the test was matched with the sum of the individual flow capacities of the well's various facies types. Each facies' flow capacity was the product of the facies type's unknown permeability and its cumulative thickness in the well. The result of the match was a range of permeabilities for each facies type, two types—grainstone and wackestone+—being particularly permeable. Production logs in one well confirmed the productivity of wackestone+ (right).

A much earlier study, predating imaging technology, also recognized clear differences in permeabilities of the rock types of the Dunham classification. This study first



□ **Matching well tests with Dunham-style evaluation in an Indian offshore carbonate field to provide permeability values for main facies types. Cumulative flow profile (left) and flow contribution from each layer (middle) confirm high permeability of wackestone+ (right).**

9. Vashist N, Dennis RN, Rajvanshi AK, Taneja HR, Walia RK and Sharma PK: "Reservoir Facies and Their Distribution in a Heterogeneous Carbonate Reservoir: An Integrated Approach," paper SPE 26498, presented at the 68th SPE Annual Technical Conference and Exhibition, Houston, Texas, USA, October 3-6, 1993.

10. Choquette PW and Pray LC: "Geologic Nomenclature and Classification of Porosity in Sedimentary Carbonates," AAPG Bulletin 54 (February 1970): 207-250.

11. Ayan C, Colley N, Cowan G, Ezekwe E, Goode P, Halford F, Joseph J, Mongini A, Obondoko G, Pop J and Wannell M: "Measuring Permeability Anisotropy: The Latest Approach," Oilfield Review 6, no. 4 (October 1994): 24-35.

used a rudimentary log interpretation method to distinguish one rock type from another (*below, left*).¹² Once the type was identified, a relevant porosity-permeability relationship was applied at each depth to calculate permeability from porosity logs. The procedure resulted in far better agreement with core permeability measurements than had previously been obtained.

In general, there are two ways to establish elusive petrophysical parameters such as permeability from log data. One is to link the parameter statistically to log data, calibrating the link with measurements of the parameter made in the field or laboratory. The calibration can be in just one well or an entire field. An example is the Indian offshore study where well test results were linked to a statistically derived facies interpretation. The variety of such statistical methods is immense

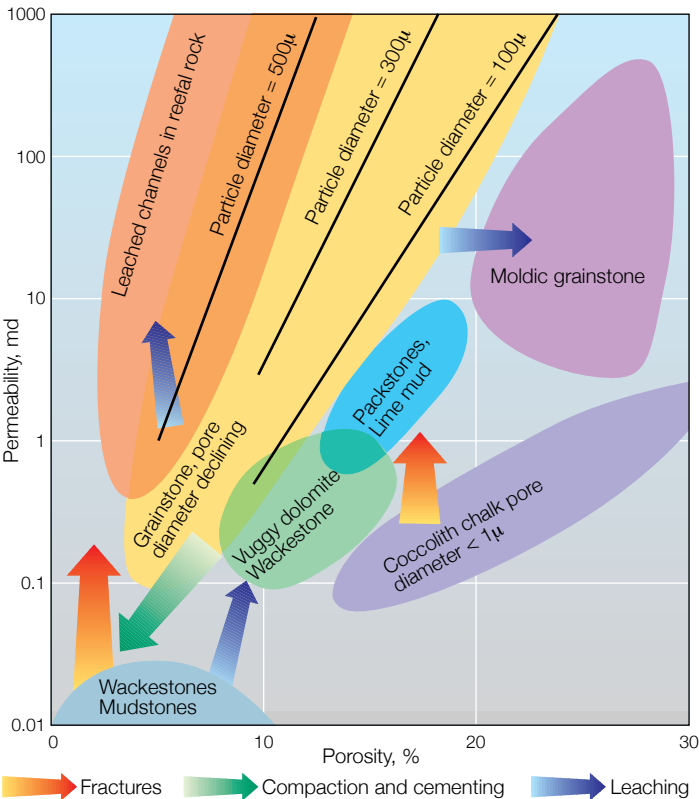
and currently extends to the use of neural networks that attempt to mimic and even improve on our inherent ability to recognize patterns in diverse data.¹³

The other approach is to somehow directly measure something about the rock's pore space, ideally from logs, and then tie this in with sought-after petrophysical parameters such as saturation and permeability. To this end, the newest measure comes from FMI images, again thanks to SPOT processing. The proportion of an image delineated as pore space leads directly to a new estimate of porosity, subject of course to the interpretation that dark areas of the image are indeed pores.

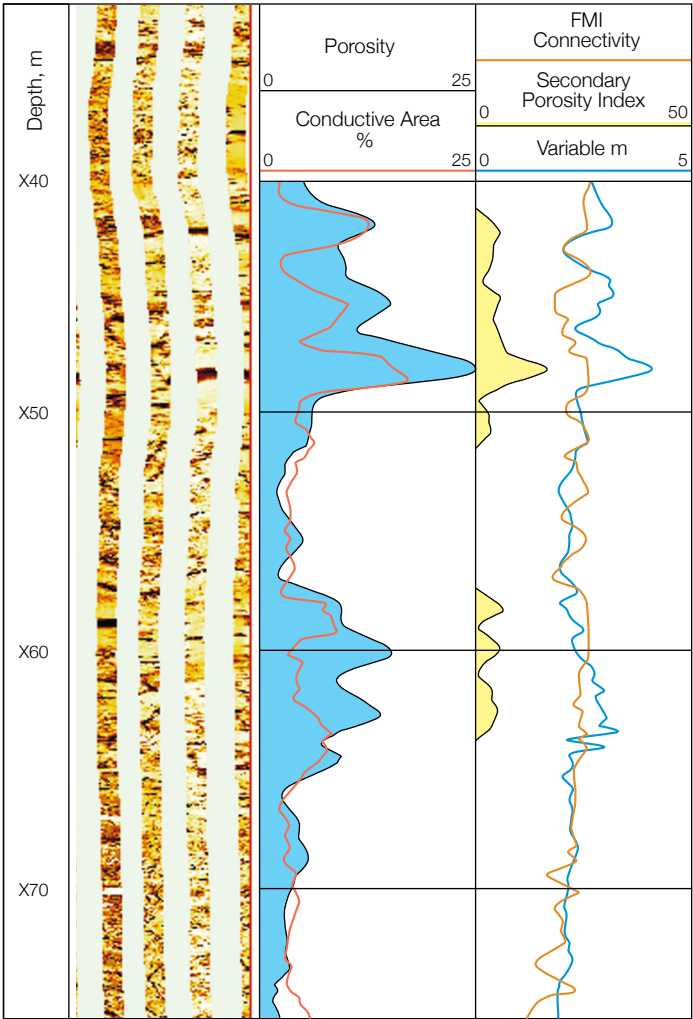
In a well drilled through a carbonate reservoir in Italy, SPOT-derived porosity compares well with porosity conventionally interpreted from neutron and density logs (*below, right*).

In much of the logged interval, the two porosities agree well, while elsewhere porosity derived from the FMI images is substantially less than conventional porosity. This could be due to the FMI tool responding only to pores larger than the 5-mm resolution of the tool and missing smaller intergranular and micritic pores. Interestingly, zones where the two porosities differ coincide with zones flagged with a secondary porosity index by the SPOT interpretation.

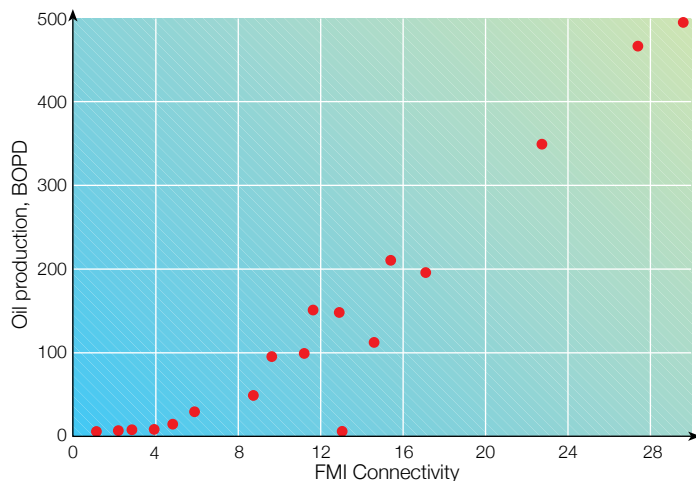
Another SPOT calculation is connectivity, an elaborately conceived but necessarily limited attempt to quantify the degree of connection between pores identified on images. A limitation is imposed because two-dimensional images can say only so much about three-dimensional connectivity. Nevertheless, SPOT connectivity has successfully predicted the productivity of oil



□ Permeability-porosity relationships for carbonate rocks following Dunham classification.



□ From a carbonate field in Italy: an FMI image (left track) allows SPOT calculation of percentage area of conductive objects. Comparison (middle track) between SPOT porosity (orange curve) and neutron-density porosity (black curve) shows good agreement. Archie's exponent "m" (blue curve), computed from R_{xo} and EPT Electromagnetic Propagation Tool logs, and connectivity of pore space computed from FMI image (gold curve) also correlate (right track), except where there is secondary porosity (yellow).



and gas wells in Texan and Oklahoman Ordovician carbonates with vuggy, connected porosity (above).

Without images, the commonest approach to pore geometry lies through consideration of Archie's law with its cementation exponent m :

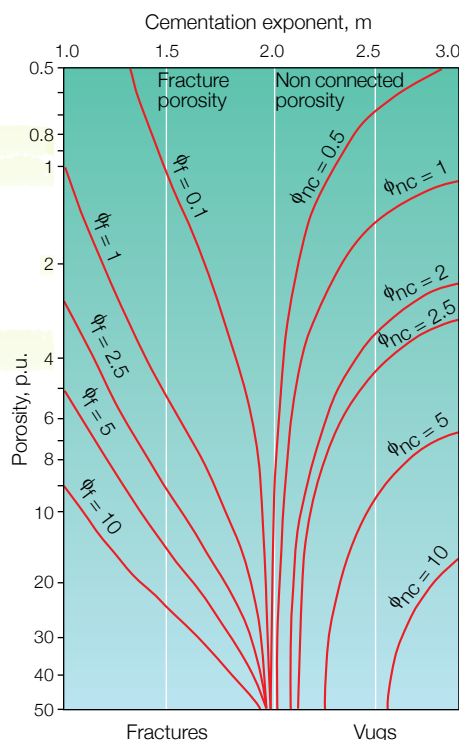
$$R_t = \frac{R_w}{\phi^m},$$

in which R_t , R_w and ϕ are, respectively, the water-filled formation resistivity, connate water resistivity and porosity.¹⁴ Early on, researchers realized that the cementation exponent captured something about the pore space, particularly its tortuosity, and thus could serve to estimate permeability as well as interpret resistivity logs. Several theoretical expressions for permeability based on m have been developed, this being a recent example:

$$k = 126.7 \phi^m R^2 \text{ millidarcies,}$$

in which R is an "effective" pore radius in microns.¹⁵

The exponent m measures reasonably constant at about 2 for sandstones, as it does for similarly constructed oolitic carbonates. But otherwise in carbonate rock, it wanders all over. In fractured carbonate rock m tends to



Conjectured variation of Archie exponent m in fractured and vuggy rocks. (Adapted from Watfa and Nurmi, reference 16.)

1, and in rocks with nonconnecting vugs m rises to 3, 4 or higher (below, left).¹⁶ A particularly copious study on Qatar carbonates by Focke and Munn shows not only how m varies with porosity—it varies a great deal—but also how that functionality depends on permeability.¹⁷ The challenge in using m to evaluate a carbonate therefore depends on being able to reliably estimate the exponent at any depth, rather than use an arbitrary value, generally 2, derived from observations on sandstones.

Guidelines for achieving this were first offered by Lucia of Shell Oil in 1981.¹⁸ Using samples from carbonate reservoirs in Texas, USA and Alberta, Canada, Lucia noted that m depended unambiguously on the proportion of the rock's porosity coming from unconnected vugs. Estimate that from core samples, he suggested, and a likely m could be derived for selected intervals in the well.

But a more versatile method was soon devised that permitted estimating m foot by foot. This made use of a new logging measurement—high-frequency electromagnetic propagation travel time, or t_{pl} .¹⁹ Like the resistivity log, t_{pl} responds to water-filled porosity, but does so without an exponent. Combining resistivity and t_{pl} therefore allows elimination of porosity for a continuous evaluation of m . The results of such an m computation transformed the accuracy of carbonate evaluation in a number of Middle East fields (next page, top). The methodology was later extended to take advantage of yet another wireline measurement, the TDT Thermal Decay Time log, permitting the continuous evaluation of not just m , but also the saturation exponent n .²⁰

The exponent n appears in Archie's law

$$R_t = \frac{R_w}{(\phi^m S_w^n)},$$

adapted for hydrocarbon-bearing rock:

12. Nurmi RD and Frisinger MR: "Synergy of Core Petrophysical Measurements, Log Data, and Rock Examination in Carbonate Reservoir Studies," paper SPE 11969, presented at the 58th SPE Annual Technical Conference and Exhibition, San Francisco, California, USA, October 5-8, 1983.

13. Wiener JM, Rogers JA, Rogers JR and Moll RF: "Predicting Carbonate Permeabilities from Wireline Logs Using a Back-Propagation Neural Network," Expanded Abstracts, SEG 61st Annual International Meeting and Exposition, Houston, Texas, USA, November 10-14, 1991: 285-288.

Mohaghegh S, Arefi R, Ameri S and Rose D: "Design and Development of an Artificial Neural Network for Estimation of Formation Permeability," paper SPE 28237, presented at the SPE Petroleum Computer Conference, Dallas, Texas, USA, July 31-August 3, 1994.

14. "Archie's Law," *The Technical Review* 36, no. 3 (July 1988): 4-13.

15. Watfa M and Youssef FZ: "An Improved Technique for Estimating Permeability in Carbonates," paper SPE 15732, presented at the 5th SPE Middle East Oil Show, Manama, Bahrain, March 7-10, 1987.

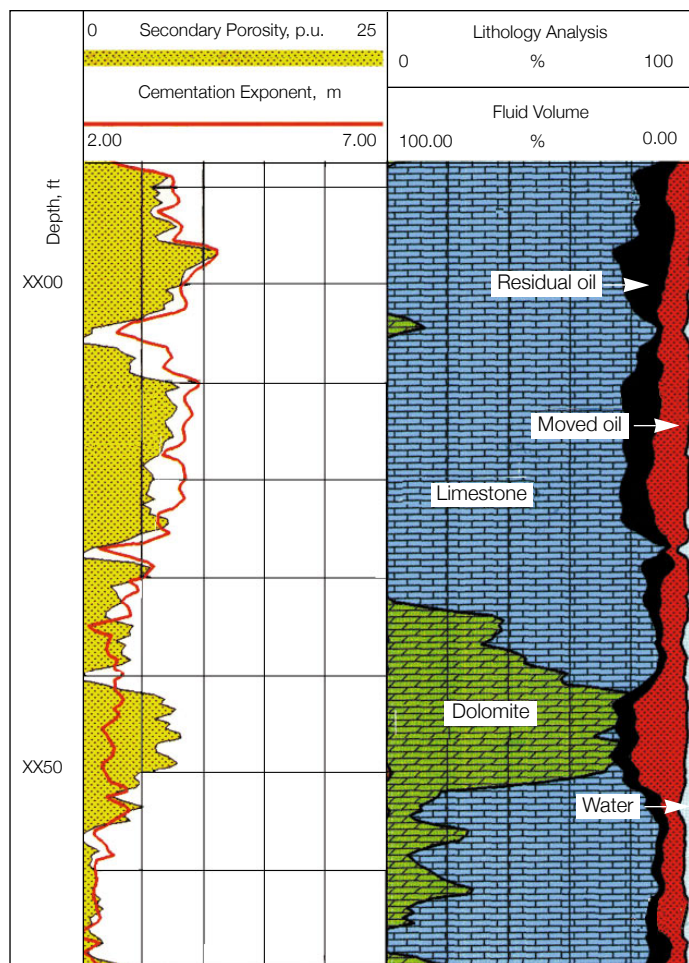
16. Watfa M and Nurmi R: "Calculation of Saturation, Secondary Porosity and Producibility in Complex Middle East Carbonate Reservoirs," *Transactions of the SPWLA 28th Annual Logging Symposium*, London, England, June 28-July 2, 1987, paper CC.

17. Focke JW and Munn D: "Cementation Exponents (m) in Middle Eastern Carbonate Reservoirs," paper SPE 13735, presented at the Middle East Oil Technical Conference and Exhibition, Bahrain, March 11-14, 1985.

18. Lucia FJ: "Petrophysical Parameters Estimated from Visual Descriptions of Carbonate Rocks: A Field Classification of Carbonate Pore Space," paper SPE 10073, presented at the 56th SPE Annual Technical Conference and Exhibition, San Antonio, Texas, USA, October 5-7, 1981.

19. Freeman DW and Henry KC: "Improved Saturation Determination with EPT," paper SPE 11466, presented at the SPE Middle East Oil Technical Conference, Manama, Bahrain, March 14-17, 1983. Amin AT, Watfa M and Awad MA: "Accurate Estimation of Water Saturations in Complex Carbonate Reservoirs," paper SPE 15714, presented at the 5th SPE Middle East Oil Show, Manama, Bahrain, March 7-10, 1987.

20. Watfa M: "Using Electrical Logs to Obtain the Saturation Exponent (n) in the Archie Equation," paper SPE 21415, presented at the SPE Middle East Oil Technical Conference and Exhibition, Bahrain, March 2-5, 1994.



□ **Archie exponent "m," determined from EPT and resistivity logs, compared with secondary porosity, determined by subtracting sonic porosity from neutron-density porosity—in the Arab carbonate formation. In the pure limestone zone at the top, the two parameters match well. In the dolomite zone at the bottom, they diverge, indicating the presence of unconnected vuggy porosity.** [Reprinted from Nurmi et al.: "Typecasting Heterogeneities," Middle East Well Evaluation Review, no. 10 (1991):16-32.]

in which S_w is water saturation. Like the exponent m , n also runs into trouble in carbonates, sometimes varying dramatically from the conventionally assumed value of 2.²¹ This has been shown in several sets of experiments on cores, the most recent by Bouvier (below).²² Petrophysicists suspect the likely cause of discrepancy is tiny micropores in the micritic matrix. Most probably, these small pores still contain original water while the large pores contain oil. It is also probable that the micrite remains water wet, while the grains have become oil wet. Both phenomena would explain why carbonate formations producing only oil sometimes exhibit low resistivities more characteristic of a water-bearing formation. Essentially, the water-filled micropores provide a short-circuit to the survey current.

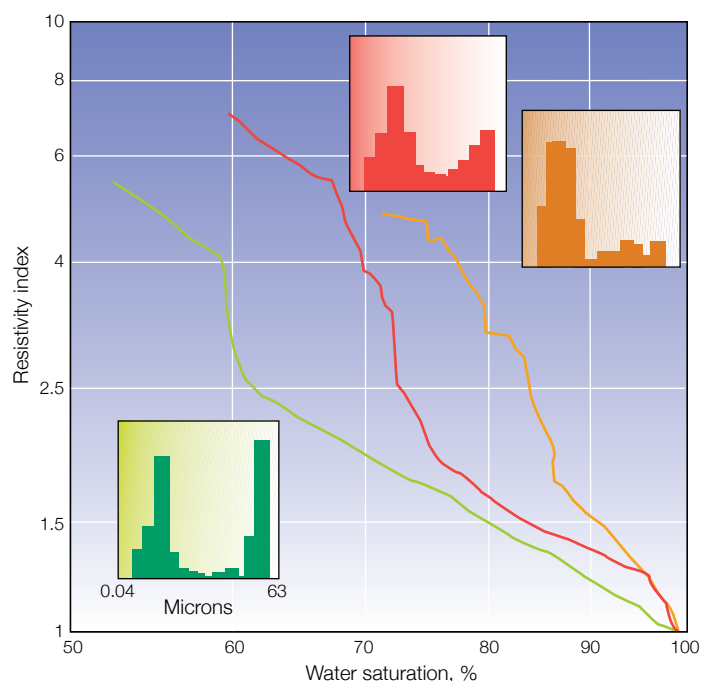
In summary, the classic Archie approach for analyzing the complex pore geometries of carbonate is fraught with obstacles, which have been only partially overcome.

New Logging Techniques

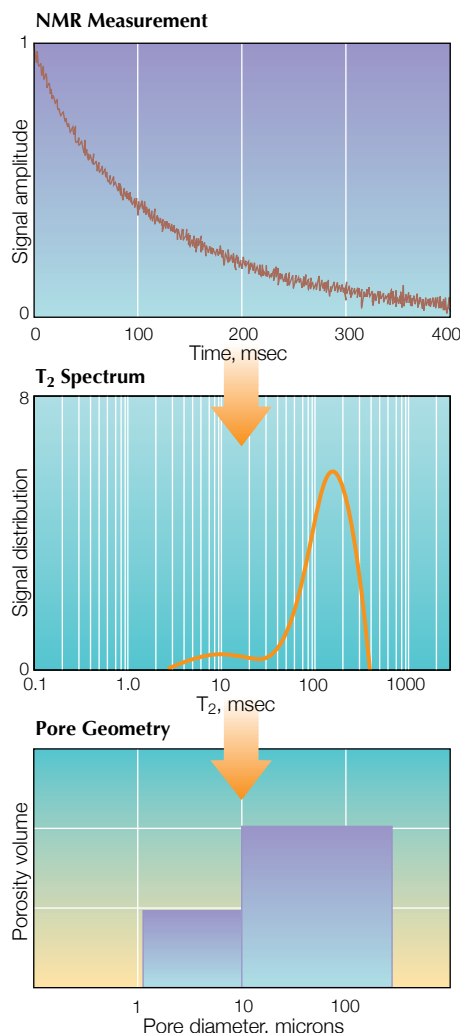
Today, two new techniques—nuclear magnetic resonance (NMR) logging and Stoneley wave logging—offer new perspectives on carbonate permeability and pore structure. The theoretical foundations for both techniques have been known for years, but until recently neither has received adequate technical implementation. That is changing with the introduction of the CMR Combinable Magnetic Resonance tool and the DSI Dipole Shear Sonic Imager tool.

In nuclear magnetic resonance, sharp magnetic pulses are used to momentarily reorient hydrogen molecules away from the ambient magnetic field direction. After each pulse subsides, the hydrogen molecules realign themselves with the ambient field, oscillating about it as they do so. Observing these oscillations permits measuring how many hydrogen molecules relax after the imposed magnetic pulse and also the rate at which they realign to the ambient field, called the relaxation.

The implications for logging are dramatic. The measurement of how many hydrogen molecules relax provides a measure of porosity, and the relaxation times indicate the size of pores containing the hydrogen molecules. Relaxation times are short in small pores because the hydrogen molecules are near the grain surface where interaction with surface charges speeds relaxation. Relaxation times are longer in large pores. Measuring the spectrum of relaxation times—so-called T_2 relaxation



□ **Carbonate rock's resistivity-versus-saturation behavior for three carbonate samples, indicating dependence on pore-size distribution. The straight-line behavior at high saturations is likely dominated by large pores, while the behavior at low saturations is dominated by small pores. Resistivity index is defined as the ratio of rock resistivity at an arbitrary saturation to rock resistivity when water saturated.** (Adapted from Bouvier, reference 22.)



□ **Decaying signal amplitude from a downhole nuclear magnetic resonance measurement (top) is transformed to a T_2 relaxation spectrum (middle), and then interpreted in terms of rock pore geometry (bottom).** (Adapted from Morriss et al., reference 23.)

times—resulting from each pulse promises to give an indication of the range of pore sizes in reservoir rock. In sandstones, comparisons between T_2 relaxation times and mercury porosimetry, a standard lab technique for evaluating pore sizes—pore neck sizes to be precise—are generally good (above).²³ This indicates that in sandstones, there is a predictable relationship between pore and pore neck sizes. Researchers are conducting similar measurements on carbonates, but results so far have not shown the same predictable relationship.

The CMR measurement is made from a pad-type tool with permanent magnets that provide an ambient field focused entirely into

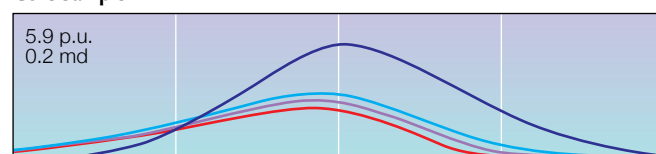
the formation. This rules out the possibility of a borehole signal, a problem that plagued earlier technology that used instead the much weaker and unfocused earth's field. Eliminating the borehole signal used to require the expensive and unpopular technique of doping the entire mud column with magnetite. The new tool's depth of investigation is about 1 in. [2.5 cm], and a dead zone directly in front of the pad avoids most effects from mudcake or rugosity. Vertical resolution is just 6 in. [15 cm], facilitating comparisons with the high-resolution FMI logs.

Recent CMR logs run in carbonate formations in West Texas coupled with laboratory measurements on cores from the wells illustrate exciting possibilities for overall petrophysical evaluation.²⁴ The formations in question are partly dolomitized carbonates with a good deal of nonconnected vuggy porosity. In addition, silt layers create vertical permeability barriers. The main interpre-

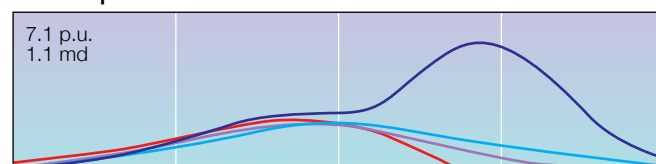
tation challenge is to estimate at any depth what percentage of porosity actually contributes to production. This requires being able to discount the minute pore space in the silt and also any vuggy porosity that is not connected.

T_2 spectra were measured on water-saturated cores both before and after they had been centrifuged to expel all producible water (below). Before centrifuging, the spectra show water-filled porosity covering the full range of pore sizes, while spectra after centrifuging no longer show the large pore sizes, since the water has been expelled from them. Equating the porosity difference between the two spectra with the volume of water expelled during centrifuging established a T_2 cutoff of 95 msec to divide large from small pores. Applying this cutoff to spectra measured by the CMR tool provided an estimate of small-pore porosity that correlated well with silt intrusions evaluated

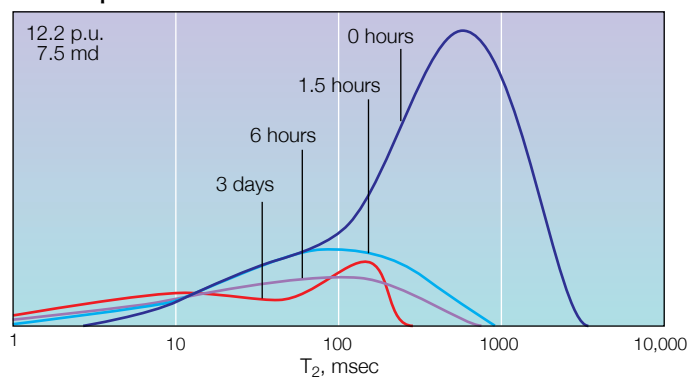
Core Sample 1



Core Sample 2



Core Sample 3



□ **T_2 spectra for three samples during laboratory centrifuging to drive water from the pores. As centrifuging continues for a total duration of three days, water is gradually expelled from large pores, leaving some water in the small ones.**

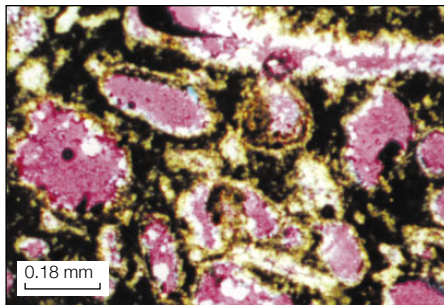
21. "Archie II: Electrical Conduction in Hydrocarbon-Bearing Rock," *The Technical Review* 36, no. 4 (October 1988): 12-21.
22. Bouvier L: "Les Saturations en Réservoir Carbonaté à Double Porosité: Réconciliation des Mesures Laboratoires et Diagraphiques," *Pétrole et Techniques* 375 (October 1992): 21-24.

23. Morriss CE, MacInnis J, Freedman R, Smaardyk J, Straley C, Kenyon WE, Vinegar HJ and Tutunjian PN: "Field Test of an Experimental Pulsed Nuclear Magnetism Tool," *Transactions of the SPWLA 34th Annual Logging Symposium*, June 13-16, 1993, Calgary, Alberta, Canada, paper GGG.
24. Chang D, Vinegar H, Morriss C and Straley C: "Effective Porosity, Producing Fluid and Permeability in Carbonates from NMR Logging," *Transactions of the SPWLA 35th Annual Logging Symposium*, Tulsa, Oklahoma, USA, June 19-22, 1994, paper A.

from other logs. Following visual analysis of the cores, a second cutoff at 750 msec was selected to isolate vugs from intergranular porosity. This was also applied to spectra measured downhole, providing a log of vuggy porosity (*below*).

Recent laboratory work on core samples from the carbonate Mubarraz field in Abu Dhabi, UAE, confirms the potential of NMR measurements.²⁵ A challenge in this area is to distinguish small micropores in the micrite matrix from the much larger productive intergranular pores. Analyzing 20 samples from two wells, a team of Schlumberger and Abu Dhabi Oil Company geoscientists found that micropores were correctly identified using a relaxation time cutoff of 190 msec on laboratory-measured T_2 spectra. Furthermore, permeable grainstone facies could be distinguished from lower-permeability packstones and mudstones with a cutoff of 225 msec. Finally, the NMR data could be interpreted to give more accurate permeability estimates than those obtained from conventional porosity logs. The CMR logging tool is currently being tested in Abu Dhabi, and expectations are high that similarly impressive results will be obtained in boreholes.

Another logging tool, the DSI imager, gains direct entry to permeability by physically moving fluid through the formation. This is achieved when low-frequency tube waves—called Stoneley waves—propagate



□ **Moldic porosity** (purple). **Formerly a fossiliferous micrite, the micrite has been replaced by dolomite and the more soluble calcitic fossils dissolved to leave a moldic porosity. Upper Eocene Ocala Limestone, Florida. Gypsum plate added.**

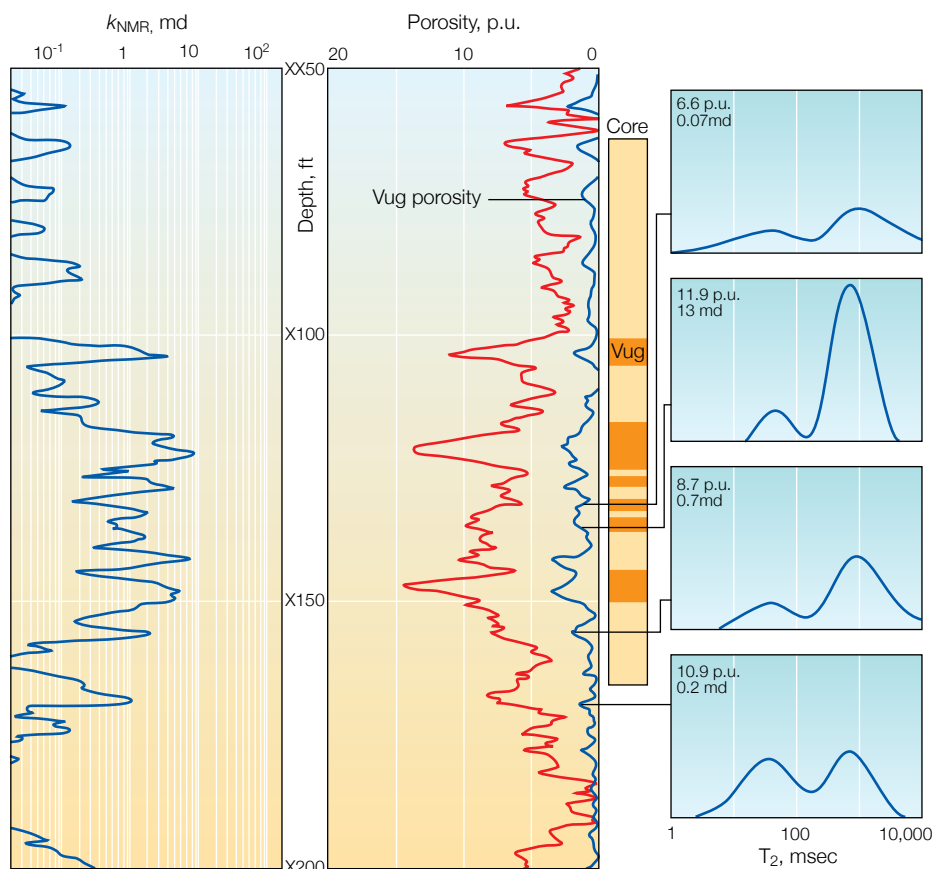
up and down the borehole. The Stoneley wave preserves most of its energy in the borehole, but in permeable formations some energy is attenuated when wave pressure pushes fluid from the borehole into the formation, similar to a quick, small-scale well test. This slows the velocity of the wave by an amount that can be related to the ratio of formation permeability to fluid

viscosity. Given a viscosity for the borehole fluid, in well-controlled circumstances such as laboratory measurements or boreholes with no mudcake, the permeability can then be estimated.²⁶

The DSI tool generates Stoneley waves with a special monopole transmitter at frequencies of 600 Hz to 5 kHz, ideal for tube-wave logging and a quantum leap ahead of previous technology equipped with transmitters operating in the 10 to 20 kHz range. Recent estimation of permeability using Stoneley-wave velocity as obtained from the DSI tool shows impressive agreement with core permeability measurements in an Abu Dhabi carbonate reservoir (*next page, top right*).²⁷

The method of obtaining permeability using Stoneley-wave velocity requires knowing the formation's density and shear velocity. A second method establishes permeability from the Stoneley wave without other data. This method is based on observing how permeability attenuates Stoneley-wave energy by directly comparing signals from near and far receivers.²⁸ Attenuation is

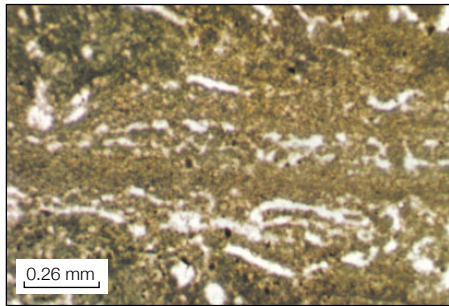
25. Kenyon WE, Takezaki H, Straley C, Sen PN, Herron M, Matteson A, Petricola MJ: "A Laboratory Study of Nuclear Magnetic Resonance Relaxation and its Relation to Depositional Texture and Petrophysical Properties—Carbonate Thamama Group, Mubarraz Field, Abu Dhabi," paper SPE 29886, presented at the SPE Middle East Technical Conference and Exhibition, Bahrain, March 11-14, 1995.
26. Winkler KW, Liu H-L and Johnson DL: "Permeability and Borehole Stoneley Waves: Comparison Between Experiment and Theory," *Geophysics* 54 (January 1989): 66-75.
27. Petricola M and Frignet B: "A Synergetic Approach to Fracture and Permeability Evaluation from Logs," paper SPE 24529, presented at the 5th Abu Dhabi Petroleum Conference and Exhibition, Abu Dhabi, UAE, May 18-20, 1992.
28. Cassell B, Badri M and Faulhaber J: "Permeability Prediction Based on Anelastic Attenuation Using Dipole Shear and Low Frequency Monopole Sources in a Carbonate Reservoir in Saudi Arabia," presented at the GEO-94 Middle East Geosciences Exhibition & Conference, Bahrain, April 25-27, 1994.



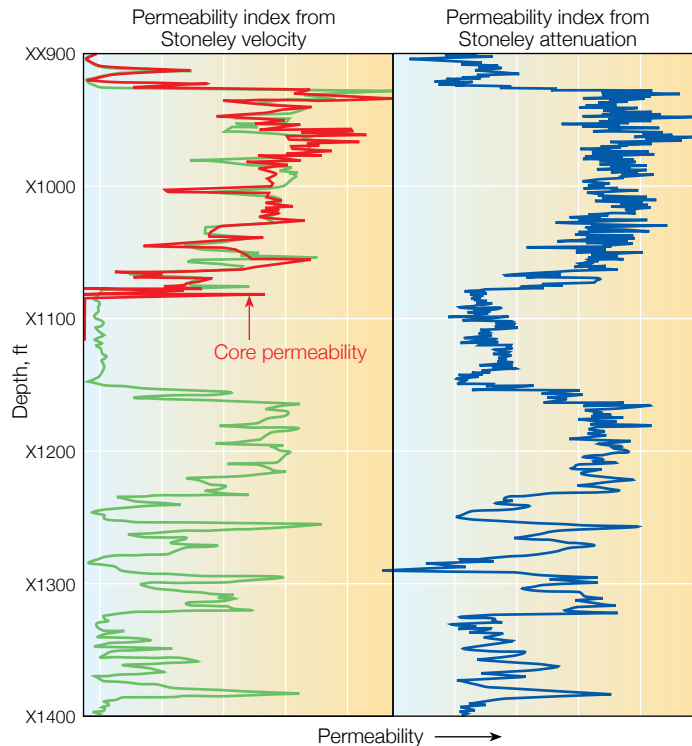
□ **T_2 spectra for vuggy carbonates showing dual-porosity system, and a log of vuggy porosity obtained from evaluating the right end of the NMR spectra only, above a cutoff of 750 msec.**

greater at higher frequencies, so the comparison is more sensitive if measured at the high end of the Stoneley-wave frequency spectrum. Excellent agreement has been observed in Middle East carbonate reservoirs between permeability estimates obtained using this second method and production logs and core data (*bottom*).

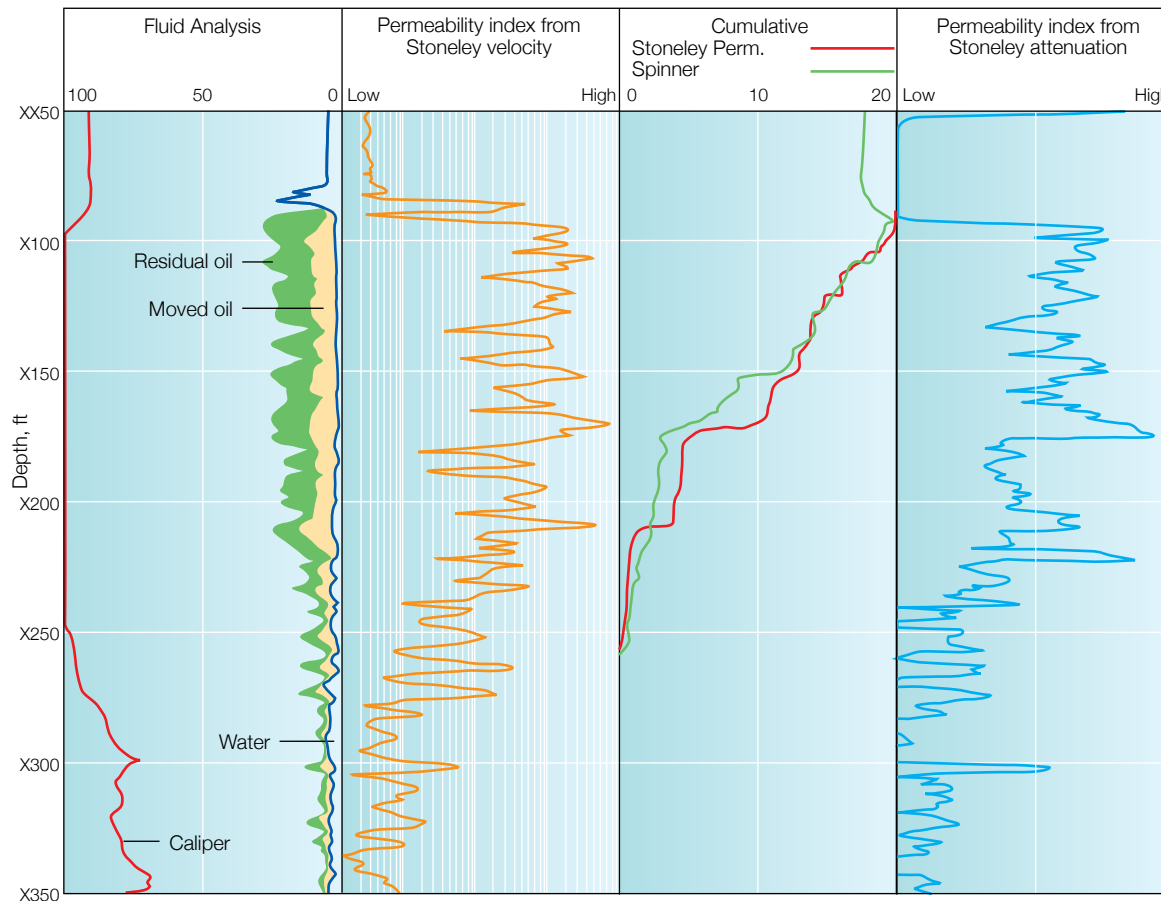
Research continues into improving Stoneley-wave permeability, for example in



□ Filled fenestral porosity in a blue-green algal biolithite. Porosity may be due to air spaces in crinkled mat sediments. Upper Silurian Limestone, Pennsylvania, USA.



□ Permeability evaluated from Stoneley-wave velocity and attenuation compared with core measurements in a Middle East carbonate reservoir. Evaluation using velocity requires formation density and shear-velocity measurements.



□ Permeability estimated from Stoneley-wave attenuation without recourse to other log data, compared with permeability from Stoneley-wave velocity, in a Middle East carbonate reservoir. Integrated permeability shows an excellent match with a flowmeter production log.

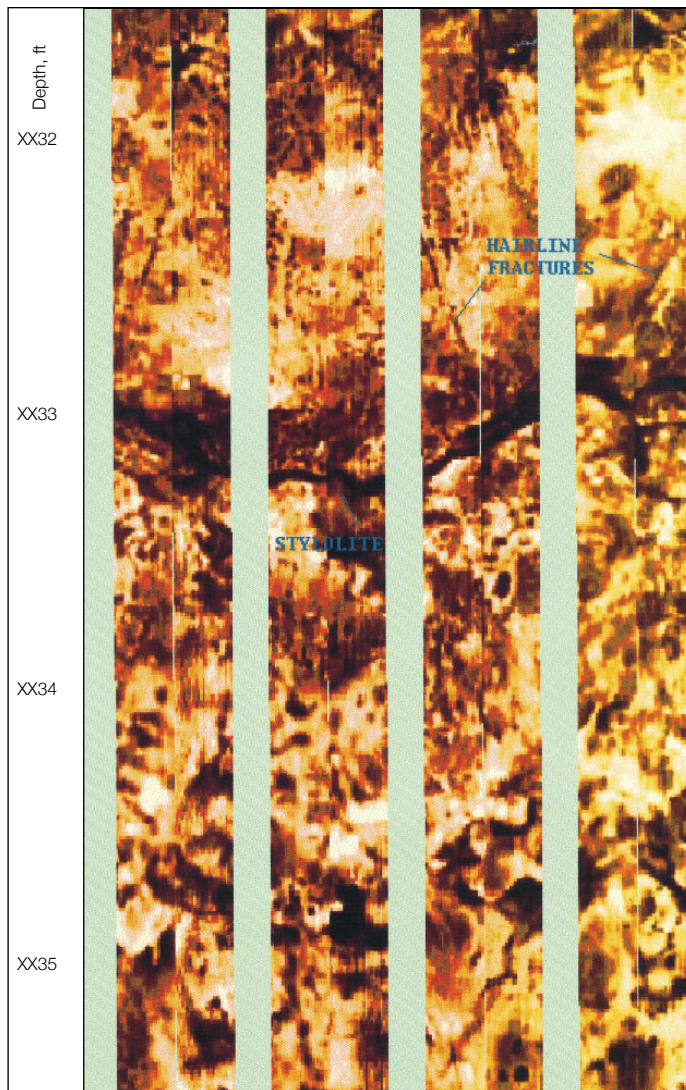
accounting for the presence of mudcake, which almost certainly interferes with the tube wave's ability to move formation fluids.

Large-Scale Features

Mapping reservoirs at the large scale and understanding their complex petrophysics at the small scale are all part of the challenge facing reservoir geologists and engineers. But in carbonates, additional care must be taken to recognize and evaluate two types of medium- to large-scale features that are caused by overburden and tectonic stresses. Either can dramatically affect reservoir performance, creating heterogeneous or anisotropic behavior where none might otherwise be suspected. These two features are stylolites and fractures.²⁹

Stylolites occur in any sedimentary formation, but are particularly common in carbonates—picture the thin, sawtooth “veins” visible on polished marble tiles and floors. Stylolites are easily recognized on outcrops and cores as irregular planes of discontinuity between rock units. Formed during compaction, probably through the mechanism of pressure solution, stylolites concentrate fine-grained insoluble residue along their irregular seams. They are usually assumed to act as permeability barriers, but some core measurement results confirm that stylolites can develop permeability. Identifying them and evaluating their impact on permeability are therefore top priorities for the reservoir engineer.

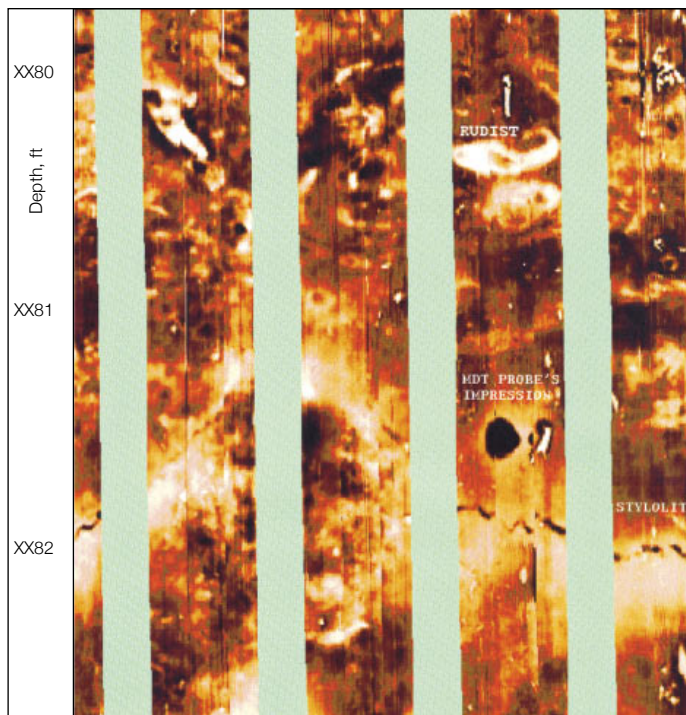
Borehole imaging has greatly facilitated the identification of stylolites downhole (right and next page). Viewed with the FMI



□ Three types of stylolites identifiable on FMI images. Dark colored stylolites (left), probably filled with clay; stylolites associated with a light band (below), are probably resistive calcite. Some stylolites are associated with extensional fractures (next page, left).

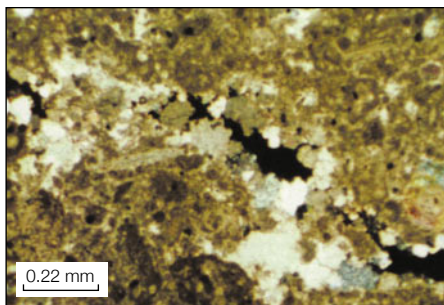


□ Filled shelter porosity beneath a large mollusk fragment. Pliocene and Pleistocene Marl, Florida.



tool, they appear in three common varieties. First, some stylolites exhibit undulating but slightly irregular surfaces and are filled with dark, therefore conductive material, probably clay. A second group of stylolites seems to have an associated band of light color, most likely resistive calcite. The third type of stylolite clearly shows associated extensional fractures caused by excessive overburden stress.

The question remains: Which stylolites form permeability barriers and which do not? Until recently, there has been no sure way of deciding. Now, answers are obtainable from a third-generation wireline testing tool, the MDT Modular Formation Dynamics Tester tool. Unlike previous wireline testers, this tool permits testing between probes set as far apart as 8 ft [2.4 m], a large



□ **Reduced fracture porosity (black).**
Upper Jurassic Limestone, Germany.
Cross-polarized light photograph.

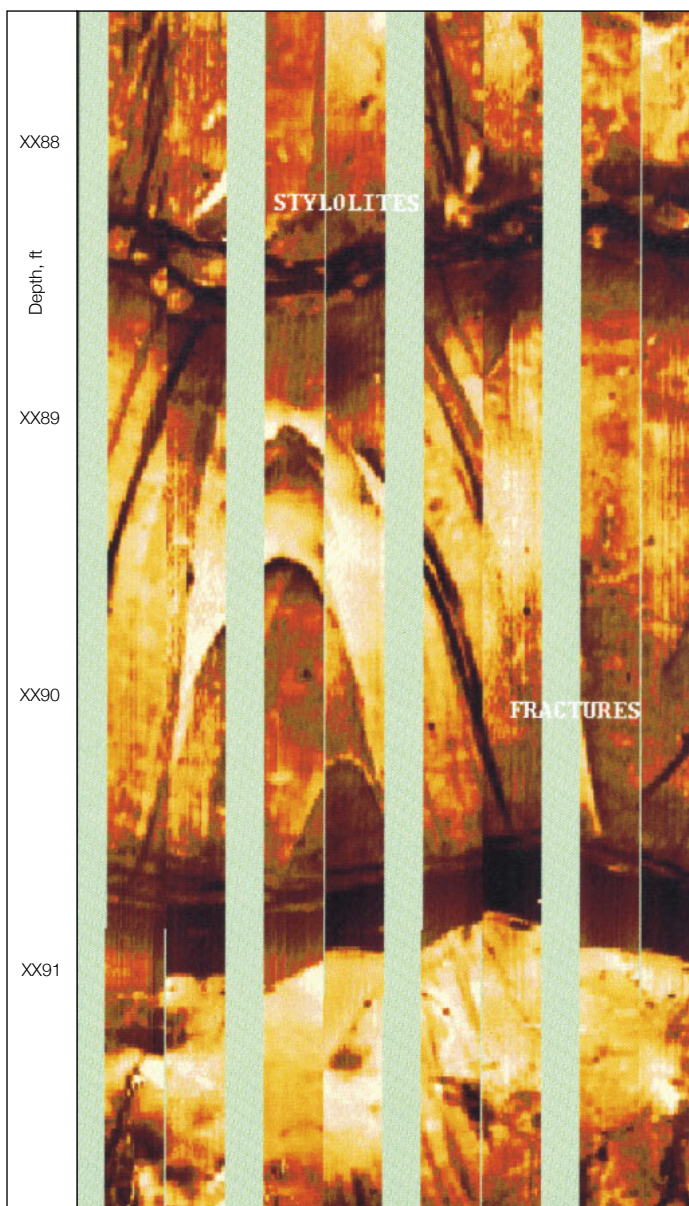
enough interval to comfortably straddle a stylolite. In such tests recently performed in the Middle East, MDT measurements indicated that stylolites previously assumed to be completely impermeable may in fact be

partly conductive to fluid flow.

If stylolites generally impede flow, fractures almost always enhance it. Indeed, some reservoirs, particularly carbonate ones, rely exclusively on fractures to achieve commercial levels of production. Before the advent of wireline imaging techniques, detecting fractures was difficult and characterizing anything about them was almost impossible. That bleak outlook changed dramatically with the introduction of the FMI and DSI tools. The recently introduced ARI Azimuthal Resistivity Imager tool also makes an important contribution in fracture detection.

Briefly, all three tools contribute to fracture interpretation, but each alone may not provide a complete picture.³⁰ On FMI images, open fractures filled with invading water-base mud of high conductivity are recognizable as dark and usually fragmented sinusoid traces. With the help of interactive FracView image processing, the interpreter can reliably pinpoint fractures, calculate their dip and azimuth, and estimate spatial density at the borehole. Additional analysis of image resistivity near the fracture can also lead to an estimation of fracture aperture.³¹

With simple models of fracture geometry, the combined log information may provide an effective fracture permeability. This can then be integrated with permeability estimates for the unfractured part of the rock to yield a permeability for the whole rock. In

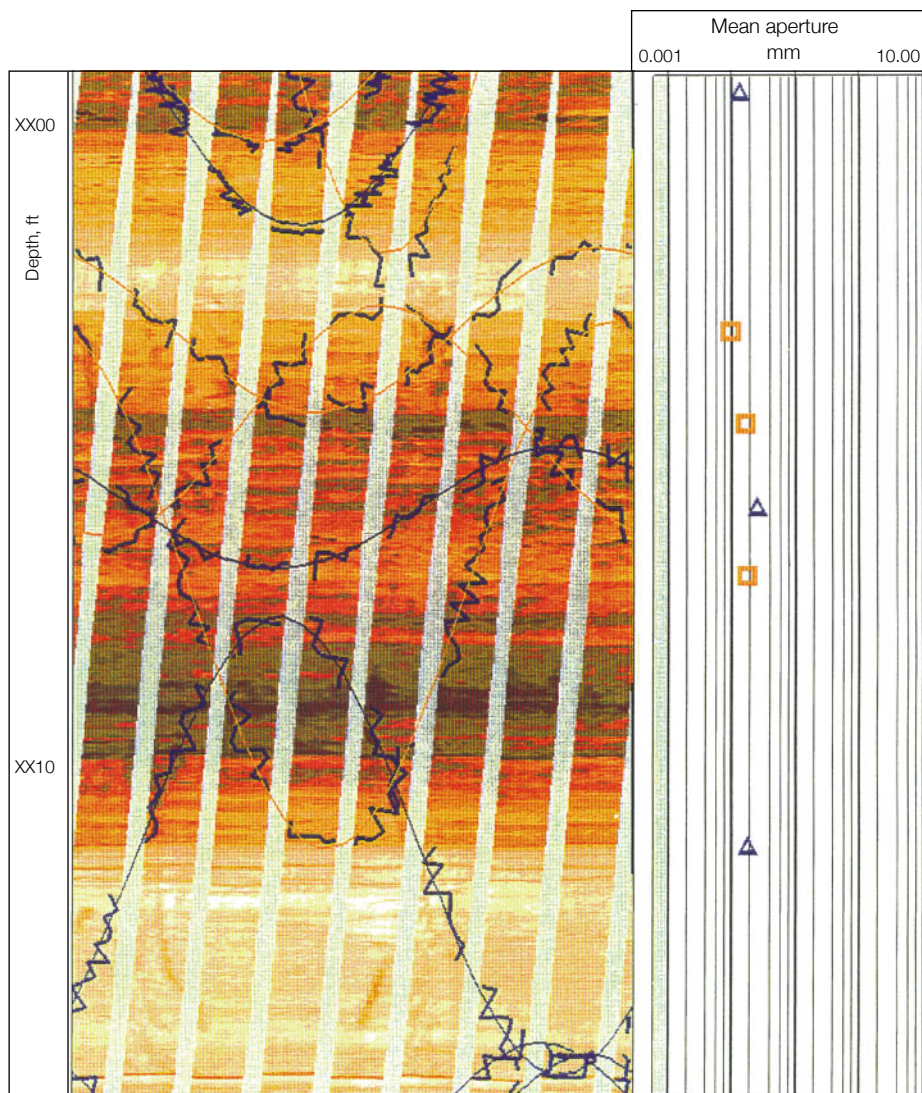


29. For general reference:

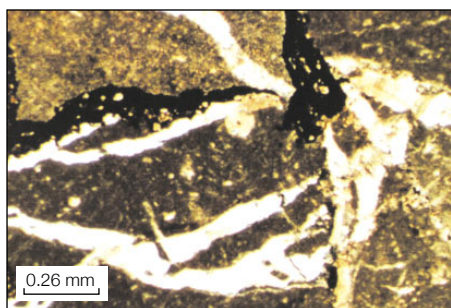
Nelson RA: "Analysis of Anisotropic Reservoirs," in *Geologic Analysis of Naturally Fractured Reservoirs*. Houston, Texas, USA: Gulf Publishing Company, 1985.

30. Cheung PS-Y and Heliot D: "Workstation-Based Fracture Evaluation Using Borehole Images," paper SPE 20573, presented at the 65th SPE Annual Technical Conference and Exhibition, New Orleans, Louisiana, USA, September 23-26, 1990.

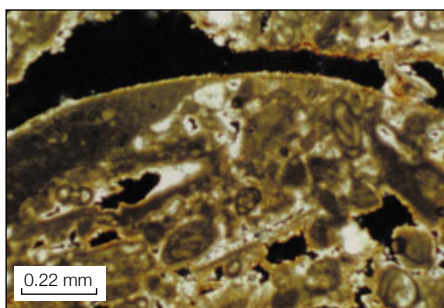
31. Luthi SM and Souhaité P: "Fracture Apertures from Electrical Borehole Scans," *Geophysics* 55 (July 1990): 821-833.



□ **Fracture evaluation and estimation of fracture aperture from an FMI image in a Rocky Mountain carbonate reservoir.** This information was used to derive an effective permeability that matched well test data. Squares and triangles signify a level of confidence in fracture identification, with squares having a higher level than triangles.



□ **Filled fracture porosity, with conjugate set of large fracture veins.** Middle Ordovician Limestone, Pennsylvania.



□ **Enlarged moldic porosity (black).** Note large mollusk mold with upper edge enlarged. Other grains include mainly miliolid foraminifera. Upper Oligocene Limestone, Florida. Cross-polarized light photograph.

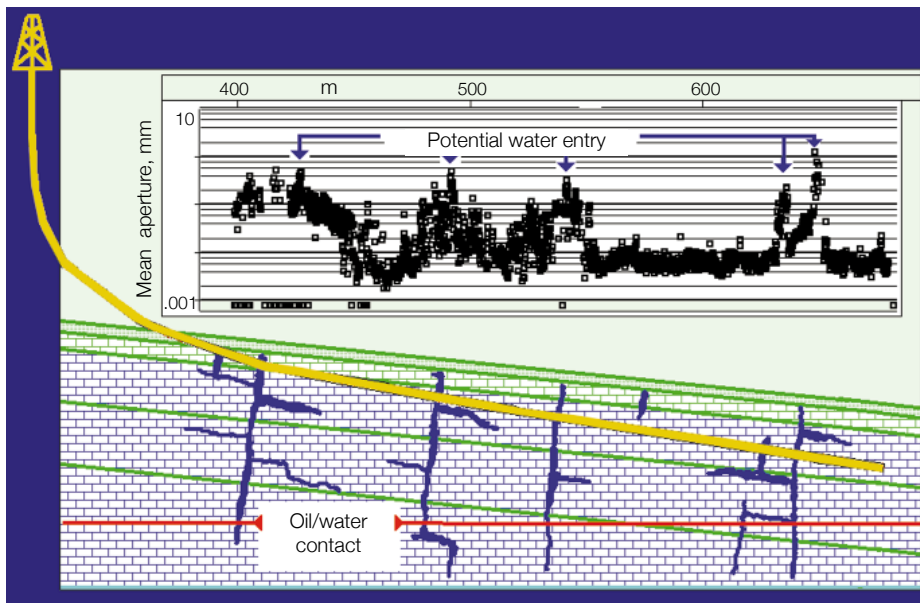
the Rocky Mountains, where a low-porosity carbonate reservoir depends on fractures for production, such a combined permeability has been successfully compared to permeability obtained from drill-stem tests (*left*).

There are a few caveats, however, to fracture interpretation using FMI resistivity images. First, the calculated fracture aperture seems to be influenced by the fluid originally filling the fracture—fractures in water zones appear systematically wider than nearby fractures in hydrocarbon zones. It is suspected that invasion fails to remove all hydrocarbon from the walls of the fracture, thereby making the fracture look thinner to electrical imaging techniques.³² In a depleted carbonate field being exploited for additional oil using horizontal wells, this phenomenon has been put to good use in identifying fractures that are likely to allow water breakthrough (*next page*).

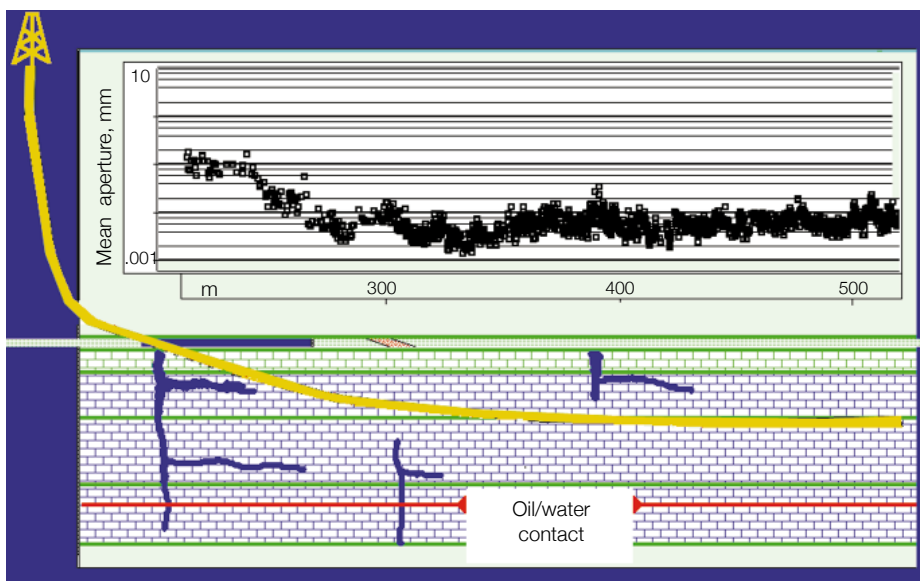
Second, the FMI tool is a relatively shallow measurement, and this limits the tool's ability to distinguish natural fractures that contribute to reservoir performance from drilling-induced fractures that do not. Certain types of drilling-induced fractures are easily recognized by their geometry—for example, vertical fractures oriented perpendicular to the least horizontal stress and therefore intersecting a vertical borehole over a lengthy interval. Nonvertical drilling-induced fractures, however, are harder to distinguish and may be easily confused with the natural variety. Fracture identification in highly deviated and horizontal wells becomes harder still.

The ARI tool provides some added depth of investigation but a poorer along-borehole resolution, and as a result, fewer fractures are detected. However, ARI image processing provides some clue to fracture depth as well as aperture, although neither is unambiguously determined.³³ The two parameters are genetically linked, so the tool response to a fracture enables an estimate of one of the parameters once a value for the other is taken.

Greater depth of investigation, up to several meters, is provided by the DSI tool that detects open fractures in the same way that it senses a permeable formation—by employing the Stoneley wave to physically pulse mud into and out of the fracture.³⁴ However, there is a commensurate deterioration in resolution along the borehole axis, to about 1.5 m [4.9 ft], showing closely spaced fractures as a single fracture. Like the FMI measurement, the Stoneley wave permits the evaluation of fracture aperture, though again this may actually represent the



□ Fracture apertures determined from FMI images in two subhorizontal wells in a fractured and partly depleted reservoir. The apertures in the top example show four zones where aperture is higher than elsewhere. This was interpreted to indicate the fractures are water-filled and liable to water out early. After completion, the top well produced with 50% water cut; the bottom well produced no water.



cumulative apertures of several neighboring fractures. Comparisons between fracture aperture estimated from the two techniques have shown good agreement in metamorphic volcanics at a UK waste disposal site. On the down side, the Stoneley wave yields no information on fracture dip or azimuth.

There may be further to go in fracture interpretation, but a comparison between the techniques of ten years ago and those of today reveals the extraordinary advances achieved by novel wireline technology and a spirited community of interpreters. It is a level of improvement common to all areas of carbonate interpretation. Today's exploitation in increasingly complex and difficult reservoirs has gained from a veritable revolution in formation evaluation. Long may it continue.

—HE, LS

32. Standen E, Nurmi R, ElWazeer F and Ozkanli M: "Quantitative Applications of Wellbore Images to Reservoir Analysis," *Transactions of the SPWLA 34th Annual Logging Symposium*, Calgary, Alberta, Canada, June 13-16, 1993, paper EEE.
33. Faivre O: "Fracture Evaluation from Quantitative Azimuthal Resistivities," paper SPE 26434, presented at the 68th SPE Annual Technical Conference and Exhibition, Houston, Texas, USA, October 3-6, 1993.
34. Hornby BE, Johnson DL, Winkler KW and Plumb RA: "Fracture Evaluation Using Reflected Stoneley-Wave Arrivals," *Geophysics* 54 (October 1989): 1274-1288.